

PARTICLE BEHAVIOUR IN NEWTONIAN AND NON-NEWTONIAN LIQUIDS

PHENOMONOLOGICAL BEHAVIOUR OF PARTICLES
IN NEWTONIAN AND NON-NEWTONIAN LIQUIDS

by

Eric Bartram, B.Sc. (Hons). Salford University, England.

A thesis submitted to the Faculty of Graduate
Studies and Research, of McGill University in
partial fulfilment of the requirement for the
degree of Master of Science.

Department of Chemistry
McGill University
Montreal, Canada

August, 1973.

ACKNOWLEDGEMENTS

The author wishes to express his sincere thanks to
Dr. S.G. Mason
for his unfailing interest and direction during the course
of this work.

Grateful acknowledgement is also made to:

Dr. H.L. Goldsmith for generous advice and assistance
in preparing this thesis.

Mr. M. Ryan for help in characterization of the
polymer solutions.

Mr. W. Poar for experimental assistance in the
design and execution of some of the investigations.

Miss G. von Chamier and Mrs. G. Brunet for typing
this thesis.

The Spruce Falls Pulp and Power Company for a
Scholarship during the session 1971-72.

The Pulp and Paper Research Institute of Canada for
laboratory accomodation and equipment and for use of the
technical facilities.


Last, but not least, my fellow students and
colleagues for their encouragement and friendship.

ABSTRACT

The behaviour of rigid and miscible deformable particles suspended in Newtonian and non-Newtonian liquids undergoing slow Couette flow was investigated. The rotations of rods and discs in pseudoplastic liquids were in quantitative agreement with the equations derived by Jeffery, whereas the particles suspended in viscoelastic fluids were not. Rotational orbits, C , drifted to limiting values, corresponding to minimum energy dissipation, in pseudoplastic liquids. However, in viscoelastic liquids discs drifted in orbit constant where $0 < C < \infty$ and, although periodic, varied from a maximum at $\phi_1 = 0, \pi$ and a minimum at $\phi_1 = \pi/2, 3\pi/2$. Also in viscoelastic liquids, under certain conditions, both rods and discs assumed a steady orientation aligned with the flow and without rotation.

A theory predicting the behaviour of miscible drops ($\sigma_{12} = 0$) in Newtonian systems was found to be in fair agreement with experimental results. A novel deformation phenomenon was found for viscoelastic systems where the interfacial tension was zero.

A speculative explanation involving the rheological properties of the fluids is advanced to explain the phenomena outlined above.



RESUME

Le comportement de particules rigides ainsi que de particules miscibles et déformables, en suspension dans des liquides Newtoniens et non-Newtoniens, et subissant un courant de Couette lent, a été exploré. Les rotations de disques et de tiges dans des liquides pseudoplastiques sont, du point de vue quantitatif, en bon accord avec les équations dérivées par Jeffery, tandis que les particules en suspension dans des liquides viscoélastiques ne le sont pas. Dans les liquides pseudoplastiques les orbites de rotation se modifient jusqu'à des valeurs limites, correspondant à une perte d'énergie minimum. Cependant, dans les liquides viscoélastiques les disques modifient leur constante orbitale C telle que $0 < C < \infty$, constante qui bien que périodique, varie d'un maximum à $\phi_1 = 0, \pi$ à un minimum à $\phi_1 = \pi/2, 3\pi/2$. De plus dans les liquides viscoélastiques et dans certaines conditions, et les disques et les tiges conservent une orientation stable, alignés dans le sens du courant et sans rotation. Une théorie prédisant le comportement de gouttes miscibles ($\sigma_{12} = 0$) dans des systèmes Newtoniens, semble en bon accord avec les résultats expérimentaux. Un nouveau phénomène de déformation a été découvert dans le cas des systèmes viscoélastiques, alors que la tension de l'interface est zéro. Afin d'expliquer les phénomènes abordés ci-dessus, une explication spéculative introduisant les propriétés rhéologiques des fluides est proposée.

TABLE OF CONTENTS

	<u>Page</u>
PART I	
GENERAL INTRODUCTION.....	1
REFERENCES.....	5
PART II	
RIGID PARTICLE MOTIONS IN NON-NEWTONIAN MEDIA.....	6
1. ABSTRACT.....	7
2. INTRODUCTION.....	8
3. THEORETICAL AND EXPERIMENTAL BACKGROUND.....	9
a) Angular velocities.....	12
b) Drift in orbit constant.....	15
c) Lateral migration.....	21
4. EXPERIMENTAL PART.....	21
a) Apparatus.....	21
b) Fluids.....	22
c) Rheological parameters.....	23
d) Particles.....	35
5. RESULTS.....	35
a) Rotation of discs in 2.5% P.A.A. solutions	36
(i) Angular velocities.....	36
(ii) Drift in orbit constant.....	36
b) Rotation of rods in viscoelastic media...	46
c) Rotation of rods and discs in shear and electric fields in 3% polyisobutylene/ decalin solution.....	58
6. CONCLUDING REMARKS.....	58

	<u>Page</u>
LIST OF SYMBOLS.....	58
REFERENCES.....	63

PART III

BEHAVIOUR OF DEFORMABLE PARTICLES IN NEWTONIAN AND NON-NEWTONIAN LIQUIDS, HAVING ZERO OR NEAR ZERO INTER- FACIAL TENSION.....	65
1. ABSTRACT.....	66
2. INTRODUCTION.....	67
3. THEORETICAL AND EXPERIMENTAL BACKGROUND.....	67
a) Deformation and orientation of drops.....	67
b) Break-up of drops.....	75
4. EXPERIMENTAL PART.....	76
a) Apparatus.....	76
b) Fluids.....	79
5. RESULTS AND DISCUSSION.....	80
a) Drop deformation in Newtonian system, $\sigma_{12}=0$	80
(i) High viscosity ratios.....	80
(ii) Low viscosity ratios.....	83
b) Drop deformation in viscoelastic systems.	83
(i) High viscosity ratios.....	86
(ii) Low viscosity ratios.....	88
c) Pseudoplastic drop in viscoelastic medium	88
6. CONCLUDING REMARKS.....	89
LIST OF SYMBOLS.....	90
REFERENCES.....	91

PART IV

1. GENERAL CONCLUSIONS.....	93
2. SUGGESTIONS FOR FURTHER WORK.....	94
3. CLAIMS TO ORIGINAL RESEARCH.....	95
REFERENCES.....	97

APPENDIX

THE COUETTE DEVICES.....	98
a) Principles.....	99
b) Description.....	100
REFERENCES.....	108

LIST OF FIGURES

<u>Figure</u>		<u>Page</u>
PART II		
1.	Cartesian coordinate systems to describe the rotation of cylinders in Couette flow and the stresses acting on the faces of a unit cube.....	10
2.	Projection of the axis of revolution of a rod on the X_2, X_3 -plane.....	17
3.	Projection of the axis of revolution of a disc on the X_2, X_3 -plane.....	19
4.	The geometry of the system for flow between eccentric rotating discs.....	25
5.	Apparent viscosity as a function of shear rate for the non-Newtonian liquids.....	28
6.	Normal stresses as a function of G for the non-Newtonian liquids.....	30
7.	Dynamic viscosity, dynamic shear storage modulus and dynamic shear loss modulus as a function of G for P.A.A. solution....	32
8.	Variation of ϕ_1 with time for a disc suspended in P.A.A. solution.....	38
9.	Equilibrium orbit of a disc, $r_p = 0.067$, as a projection of the axis of revolution on the $X_2 X_3$ plane.....	42
10.	Projection of the axis of revolution of a disc, $r_p = 0.675$, on the $X_2 X_3$ -plane.....	44
11.	Equilibrium orbits for discs of various axis ratios.....	47
12.	Equilibrium orbits for a disc, $r_e = 0.634$ at various shear rates.....	50
13.	Projection of the axis of revolution of a rod on the X_2, X_3 -plane.....	54
14.	Variation of ϕ_1 and $\sin \theta_1$ with time for a rod in P.A.A. solution.....	56

PART III

1.	Cartesian and spherical polar coordinates for the shear flow.....	69
2.	Undamped oscillations of a soluble drop; theoretical.....	73
3.	Mechanism of drop burst as observed by Rumscheidt and Mason.....	77
4.	Undamped oscillations of a soluble drops; experimental.....	81
5.	Measured deformation and orientation of a soluble drop, $\lambda = 0.5$	84
6.	Mechanism of deformation and burst for a viscoelastic system.....	87

LIST OF TABLES

Table

Page

PART III

1. Comparison of first normal stress differences 34
2. Effect of shear rate and axis ratio on period of rotation of discs..... 41
3. Equilibrium orbit constants at $\phi_1 = 0$ and $\pi/2$ as a function of axis ratio..... 49
4. Equilibrium orbit constants for a disc as a function of shear rate..... 52.

PART I

GENERAL INTRODUCTION

[Handwritten signature]

"Rheology. Study of the deformation and flow of matter in terms of stress, strain and time".¹⁾

From the above definition it can be understood that the scope of this scientific subject encompasses many disciplines. This broad definition can be broken down into two inter-related categories: (i) macrorheology, which regards all materials as homogeneous and devoid of structure, and (ii) microrheology which, from a detailed study of the behaviour of the elemental particles of which a material is composed, predicts the macroscopic rheological properties. This thesis is concerned with the study of the behaviour of individual particles suspended in elementary volumes of Newtonian and non-Newtonian liquids undergoing laminar shear flow.

The first theory for the steady rotation of rigid spheres was that given by Einstein²⁾. This was later extended by Jeffery³⁾ to include spheroids, (the relevant details of which are given in Part II). A recent theory by Cox⁴⁾ presents in a more general form, the earlier work of Taylor^{5,6)}, who described the deformation and internal circulation of fluid drops. The equations of importance to this work being described in Part III of this thesis. Goldsmith and Mason⁷⁾ have reviewed the subsequent experimental investigations carried out in this laboratory and elsewhere, along with the underlying theories, and describe the behaviour of rigid and deformable particles in Newtonian liquids undergoing Couette and Poiseuille flow at low Reynolds numbers. Since then other workers^{8,9)} here have studied the motions of particles in

non-Newtonian suspending fluids. The angular velocities of rigid particles in pseudoplastic liquids were found to be in agreement with equations derived by Jeffery³⁾, but the orbit constants of rods and discs drifted to limiting values. In viscoelastic liquids, at sufficiently high shear rates, the discs ceased to rotate and aligned themselves with the direction of the flow. Also migration of rigid particles in pseudoplastic liquids in Couette flow was towards the region of increasing velocity gradient, whereas the opposite was true in viscoelastic fluids.

Part II of this study extends this earlier work of Karnis⁸⁾ and Gauthier⁹⁾ for single rigid cylinders suspended in non-Newtonian liquids, special attention being focussed on the behaviour of particles suspended in viscoelastic liquids at shear rates greater than previously used and also the drift to an equilibrium orbit for discs having axis ratios closer to unity.

Part III deals with the behaviour of liquid drops, having zero or near zero interfacial tension with respect to the suspending medium, undergoing slow Couette flow. The theory by Cox⁴⁾ which predicts the behaviour of these particles under the above conditions when both drop and medium are Newtonian is tested experimentally, and also the deformation and burst of non-Newtonian systems are characterized.

Parts II and III have been written in a form suitable for publication and as such are complete with their own experimental and theoretical backgrounds and references.

Part IV contains the General Conclusions, Suggestions for Further Work and Claims to Original Research. The Couette devices used in this study are described in the Appendix.

REFERENCES

1. Rose, A. and Rose, E., "Condensed Chemical Dictionary" 6th Ed. (1961) Rheinhold Publishing Corp.
2. Einstein, A., "Eine neue Bestimmung der Molekuldimensionen", Ann. de Physik, 19, 289 (1906); with a correction in 34, 591 (1911).
3. Jeffery, G.V., Proc. Roy. Soc. (London), A102, 161 (1922).
4. Cox, R.G., J. Fluid Mech. 37, 601 (1969).
5. Taylor, G.I., Proc. Roy. Soc. (London), A138, 41 (1932).
6. Taylor, G.I., Proc. Roy. Soc. (London), A146, 501 (1934).
7. Goldsmith, H.L. and Mason, S.G., in Rheology: Theory and Applications (F.R. Eirich, Ed.), Vol. 4, Chapter 2, 85-250, Academic Press, New York (1967).
8. Karnis, A. and Mason, S.G., Trans. Soc. Rheol. 10, 571 (1967).
9. Gauthier, F., Goldsmith, H.L. and Mason, S.G., Rheol. Acta, 10, 344 (1971).

PART II

RIGID PARTICLE MOTIONS IN NON-NEWTONIAN MEDIA

1. ABSTRACT

Investigations of the behaviour of rigid cylinders suspended in pseudoplastic and viscoelastic liquids subject to slow Couette flow have been carried out. The results in both types of solutions showed that there was a steady drift in the orbit constant, C , to an equilibrium orbit. For the pseudoplastic media, the orbit drifts were towards an asymptotic value corresponding to minimum energy dissipation in the flow, where $C = 0$ for rods and $C = \infty$ for discs. However, discs in viscoelastic solutions of polyacrylamide drifted to an intermediate orbit with $0 < C < \infty$ which was periodic, although C continually varied between a maximum at $\phi_1 = 0, \pi$ and a minimum at $\phi_1 = \pi/2, 3\pi/2$. Furthermore, both rods and discs suspended in P.A.A., under certain conditions, aligned themselves with the flow and ceased to rotate. Also in viscoelastic media, the observed periods of rotation for cylinders were markedly greater than those given by theory.

A qualitative explanation of the above phenomena has been advanced utilizing the measured normal stress differences and elastic properties of these fluids.

2. INTRODUCTION

The theory and behaviour of rigid and deformable particles suspended in Newtonian liquids undergoing Couette or Poiseuille flow at low Reynolds numbers has been studied in this laboratory over the last 20 years¹⁾.

More recently, investigations into the behaviour of single rigid particles suspended in pseudoplastic and viscoelastic polymer solutions, subject to slow Couette flow, have also been carried out^{2,3)}. The present work extends these studies of the motions of cylinders in non-Newtonian fluids to particles having axis ratios closer to unity and to a wider range of shear rates. Qualitative observations were also made on the behaviour of conducting particles when an electric field was superimposed on the shear field.

Whereas many of the phenomena observed in Newtonian media have been theoretically predicted^{4,5,6)}, there is no such basis at present for describing certain of the particle motions in non-Newtonian fluids. Thus the migration of rigid spheres and cylinders across the planes of shear, the changes in rotational orbits of rods and discs with time and the irreversibility of two-body collisions which occur both in pseudoplastic and viscoelastic media are not observed in Newtonian fluids.

In the case of discs, which under certain conditions in viscoelastic fluids were found to align themselves without further rotation in the direction of flow³⁾, a

qualitative explanation invoking an elastic restoring torque opposing that due to viscous deformation of the fluid was advanced.

Although the present study does not give any theoretical basis for the above mentioned phenomena, it was hoped that the work would result in further qualitative understanding of the motions of rods and discs described below.

3. THEORETICAL AND EXPERIMENTAL BACKGROUND

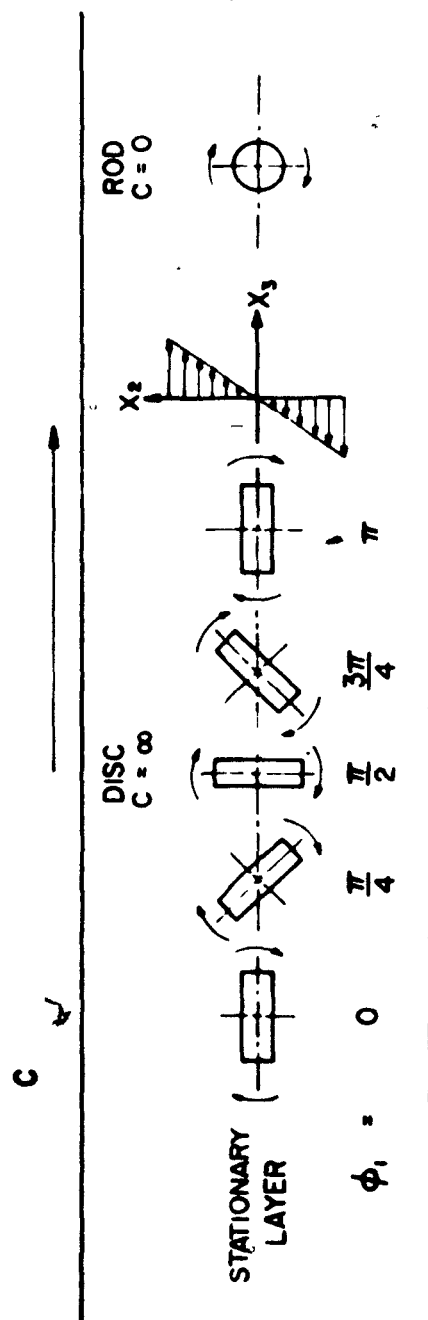
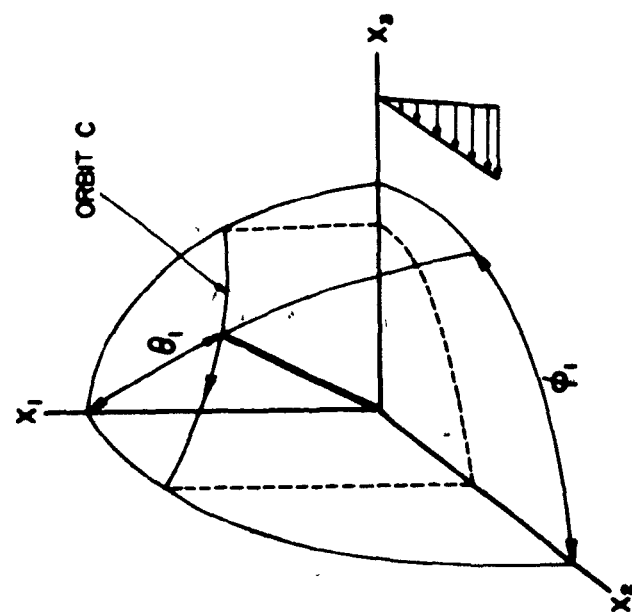
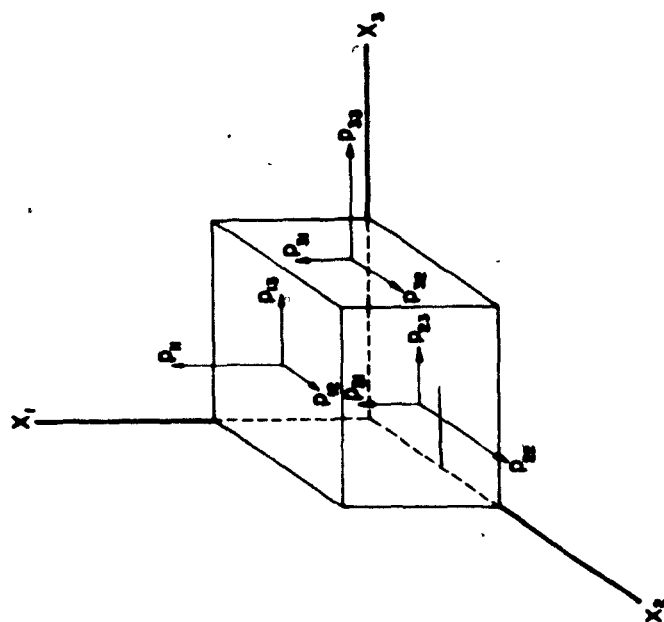
We consider the motions of single, isolated, neutrally buoyant rigid particles suspended in liquids of density ρ_0 and viscosity η_0 subjected to laminar viscous Couette flow.

An extension of the mathematical treatment by Einstein⁷⁾ concerning the increase in fluid viscosity due to the presence of suspended spheres, as well as the results of Oberbeck⁸⁾ and Edwards⁹⁾ led Jeffery⁴⁾ to formulate a set of equations describing the rotation of the axis of revolution of small ellipsoidal particles suspended in Newtonian liquids at the origin of a field of plane Couette flow $u_1 = 0, u_2 = 0, u_3 = GX_2$. Here u_1, u_2, u_3 are the respective fluid velocities along the Cartesian coordinates X_1, X_2, X_3 shown in Figure 1a, and G is the velocity gradient or shear rate. In the case of an ellipsoid of revolution (spheroid) the equations show that the movement of the axis of revolution about the polar, X_1 -axis is somewhat like the motion of a precessing top, with the angular rotation given by:

FIGURE 1

- (a) Cartesian coordinate system X_1, X_2, X_3 of the external flow field. θ_1 and ϕ_1 are the polar coordinates with respect to X_1 as the polar axis. The upper end of the axis of revolution of a prolate spheroid ($r_e > 1$) is shown tracing out the path of a spherical elliptical orbit having the orbit constant C .
- (b) Stresses acting on three faces of a unit cube in a Cartesian coordinate system X_1, X_2, X_3 ; p_{11} , p_{22} and p_{33} are the normal stress components and p_{ij} , ($i \neq j$), are the tangential (or shear) stress components.
- (c) Projections of a disc (left) and a rod (right) rotating in Couette flow viewed along the X_1 -axis after they have attained orbits having the respective limiting values $C = \infty$ and $C = 0$.

(After Gauthier, Goldsmith and Mason³.)



$$\omega_1 = \frac{d\phi_1}{dt} = \frac{G}{(r_p^2 + 1)} (r_p^2 \cos^2 \phi_1 + \sin^2 \phi_1) , \quad [1]$$

$$\frac{d\theta_1}{dt} = \frac{G(r_p^2 - 1)}{4(r_p^2 + 1)} \sin 2\phi_1 \sin 2\theta_1 . \quad [2]$$

Here ϕ_1 and θ_1 are the spherical polar angles defined in Figure 1a, r_p is the particle axis ratio (axis of revolution/equatorial diameter) = $2a/2b$.

a) Angular velocities

For the simplest case of a sphere ($a = b$), Eq. [1] reduces to

$$\omega_1 = G/2 . \quad [3]$$

The particle rotates with a constant angular velocity and has the period of rotation

$$T = 4\pi/G . \quad [4]$$

Rigid spheres suspended in Newtonian liquids¹⁰⁾ have been shown to obey Eqs. [3] and [4]. With pseudoplastic carbopol solutions which followed the power law relation;

$$p_{23} = KG^n , \quad [5]$$

p_{23} being the tangential shear stress (Figure 1b) and K and n constants depending upon the fluid. The mean observed angular velocities over a range of G from 0.13 sec^{-1} to 2.18 sec^{-1} were also in agreement with theory³⁾, provided the shear rate at the stationary layer in the annulus of the

Couette was calculated taking into account the non-Newtonian velocity profile;

$$G(R) = \frac{2}{n} \frac{\Omega_I R_I^{2/n} - \Omega_{II} R_{II}^{2/n}}{R_{II}^{2/n} - R_I^{2/n}} \quad [6]$$

Here Ω_I and Ω_{II} are the angular velocities of the inner and outer cylinders respectively, R is the radial distance from the centre of rotation and R_I and R_{II} the radii of the inner and outer cylinders respectively. When the liquid is Newtonian, $n=1$ in Eq. [6]. For the viscoelastic polyacrylamide solutions complete velocity profiles were not available, but a few measurements of the local G at the stationary layer suggested that here too $2\omega_1/G = 1$ and that the rotation of the field is equal to half the velocity gradient³⁾.

When $r_p \neq 1$, Eq. [1] indicates that the angular velocity, ω_1 , varies periodically: for a prolate spheroid, $r_p > 1$, it is at a maximum when the axis of revolution, coincident with the major axis of the particle, is at right angles to the direction of the flow ($\phi_1 = 0, \pi$), and at a minimum (but not zero) when the particle major axis is aligned with the flow ($\phi_1 = \pi/2, 3\pi/2$). For an oblate spheroid, the positions of maximum and minimum velocity are reversed, since here the axis of revolution is coincident with the particle minor axis.

The particles used in nearly all previous experimental studies were cylinders (rods and discs) and not ellipsoids. Nevertheless, it was found that Eqs. [1] and [2]

were obeyed provided an equivalent ellipsoidal axis ratio r_e was used instead of the particle axis ratio r_p : r_e is obtained from the integrated form of Eq. [1]

$$\tan \phi_1 = r_e \tan \frac{Gt}{r_e + \frac{1}{r_e}} \quad [7]$$

using the experimentally determined period of rotation T of the cylinder about the vorticity axis,

$$T = \frac{2\pi}{G} \left(r_e + \frac{1}{r_e} \right) \quad [8]$$

Experimental studies of the relationship between r_e and r_p for cylinders have also led to the following empirical relationship¹¹⁾:

$$\log_{10} r_e = 0.78 \log_{10} r_p + 0.051 \quad [9]$$

which can be used to obtain the r_e value of cylindrical particles in Newtonian liquids when TG is unknown. The r_e value obtained from this result is accurate to $\pm 5\%$ in the range $r_p = 0.1 \rightarrow 50$.

Previous work³⁾ showed that for a given particle, the values of r_e calculated from Eq. [8] were the same in Newtonian and pseudoplastic solutions of Carbopol. Moreover, the measured angular velocities $d\phi_1/dt$ in these solutions were in good agreement with those calculated from Eqs. [1] and [6]. Similar results were obtained at low shear rates with rods and discs in viscoelastic 2% aqueous polyacrylamide solution.

b) Drift in orbit constant

Upon integration, Eq. [2] becomes;

$$\tan \theta_1 = \frac{C r_e}{(r_e^2 \cos^2 \phi_1 + \sin^2 \phi_1)^{1/2}} \quad [10]$$

where C is the orbit constant which defines the eccentricity of the spherical ellipse traced out by the ends of the particle axis of revolution whose principal axes are $\tan^{-1} C r_e$ at $\phi_1 = \pi/2, 3\pi/2$, and $\tan^{-1} C$ at $\phi_1 = 0, \pi$. The orbit constant may take on any value between the limits 0 and ∞ . Experimentally, good agreement with Eq. [10] in Newtonian fluids subjected to Couette or Poiseuille flow at very low Reynolds numbers has been found^{1,12,13,14,15}, provided the particles do not sediment or interact with each other and there is no Brownian motion. Under these conditions, single rods and discs rotate indefinitely in orbits determined only by the initial conditions of release.

The value of C at any given ϕ_1 can be determined from Eq. [10] with θ_1 obtained from the projected lengths of the axis of revolution $2a'(\phi_1)$ and the equatorial diameter $2b'(\phi_1)$ of the cylinders in the X_2X_3 -plane;

$$\frac{a'(\phi_1)}{a} = \sin \theta_1, \quad [11a]$$

$$\frac{b'(\phi_1)}{b} = \cos \theta_1. \quad [11b]$$

A convenient illustration of a spherical elliptical orbit is provided by plotting the projection of the axis of

revolution $a'(\phi_1)$ in the X_2X_3 -plane. At a finite value of C , this is an ellipse of axis ratio R_{23} , given by;

$$R_{23} = \left(1 + \frac{1}{C^2}\right)^{\frac{1}{2}} \left(1 + \frac{1}{C^2 r_e^2}\right)^{-\frac{1}{2}} \quad [12]$$

When $C = \infty$, $R_{23} = 1$ and the projection is a circle whose centre represents the projection at $C = 0$. Figures 2a and 3a show a set of ellipses for various C in the case of a rod and disc respectively³⁾.

In non-Newtonian fluids, however, rods of particle axis ratios from 10 to 24^{2,3)} drifted into orbits of $C = 0$ where the particle spins about its axis of revolution aligned with the X_1 -axis (Figure 1c). Discs having r_p between 0.11 to 0.17 drifted into orbits of $C = \infty$ in which the axis of revolution rotates without spin in the X_2X_3 -plane. Plots of the projection $a'(\phi_1)$ for particles drifting into these limiting orbits, in which the dissipation of energy in Couette flow is a minimum⁴⁾, are shown in Figures 2b and 3b.

A special case of the above particle rotational behaviour in non-Newtonian fluids was reported by Gauthier³⁾ who found that above a critical shear rate, discs in 2% aqueous polyacrylamide solutions oriented themselves with their axis of revolution along the X_2 -axis, $\phi_1 = 0$, $\theta_1 = 90^\circ$ and ceased to rotate further (Figure 3c). They remained aligned with the direction of flow even when the velocity gradient was further increased. The drift in the angle θ_1 to 90° occurred even when the discs were initially in the ϕ_1 -orientation = 0° . No such behaviour was reported in the

FIGURE 2

- (a) Calculated and computer-drawn X_2X_3 -projections of the axis or revolution of a rod (= semi-major axis) with $r_e = 16.1$ in various spherical elliptical orbits whose constant C increases from 0 at the origin to the circle corresponding to $C = \infty$.
- (b) The measured projections of one end of the same rod suspended in a viscoelastic 2% P.A.A. solution ($G = 0.53 \text{ sec}^{-1}$) showing the progressive drift of orbit constant from $C' = \infty$ to C close to 0 in the direction given by the arrows. The line is the best fit of the experimental points. (after Gauthier, Goldsmith and Mason³).

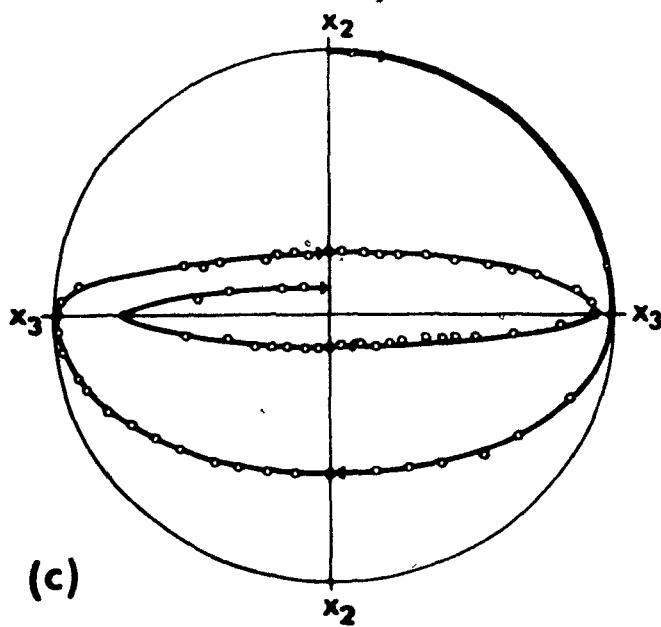
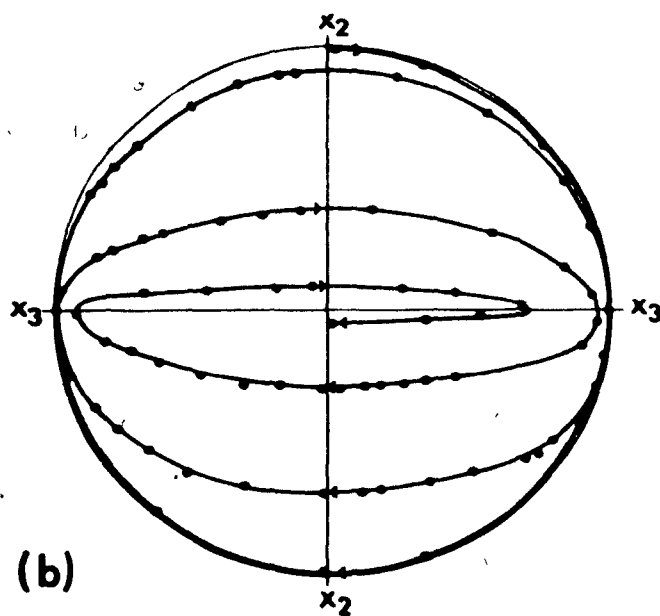
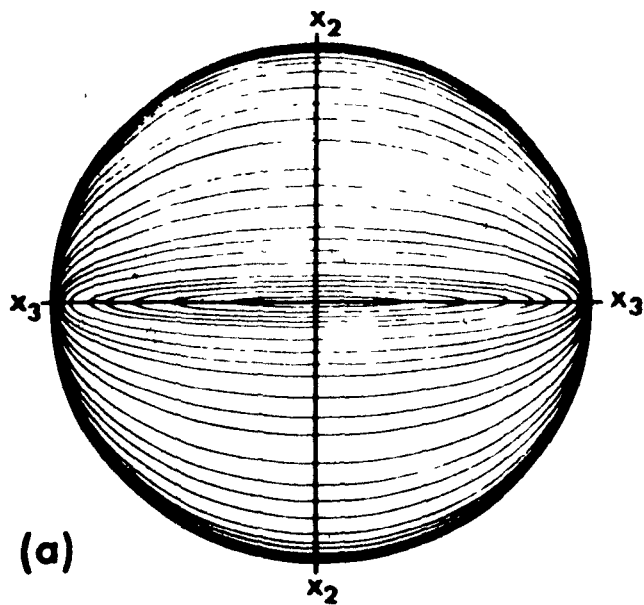
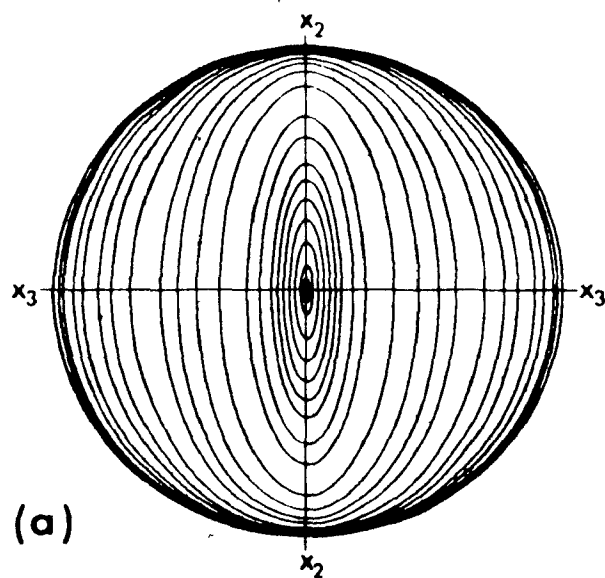


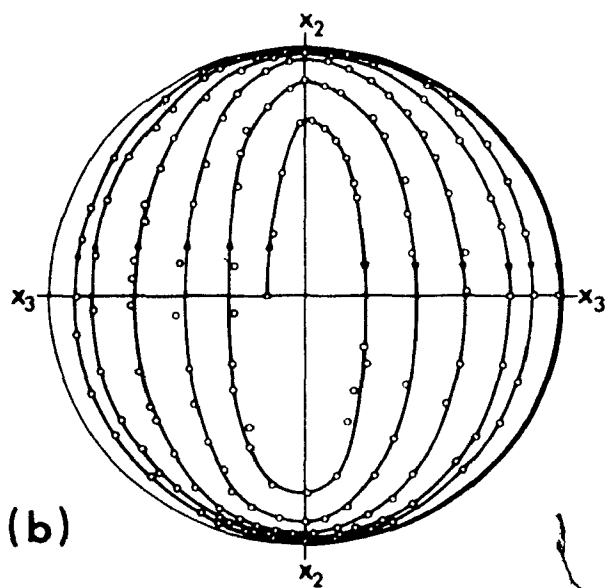
FIGURE 3

- (a) Calculated and computer-drawn X_2X_3 -projection of the axis of revolution (= semi-minor axis) of a disc with $r_e = 0.24$ rotating in various spherical elliptical orbits. At the origin $C = 0$, the circle corresponds to $C = \infty$.
- (b) Measured projections of one end of the axis of revolution of the same disc suspended in a pseudo-plastic Carbopol solution ($G_r = 1.11 \text{ sec}^{-1}$) as the orbit constant drifted from a value initially close to $C' = 0$ to $C' = \infty$ in the direction given by the arrows.
- (c) Measured projections for a disc, $r_e = 0.15$ suspended in a viscoelastic 4.0 % P.A.A. solution, showing the orientation of the particle with the axis of revolution along the X_2 -axis and where it ceased to rotate further. Open circles: $G = 1.04 \text{ sec}^{-1}$; closed circles: $G = 0.31 \text{ sec}^{-1}$. In (b) and (c), the lines are the best fit through the experimental points.

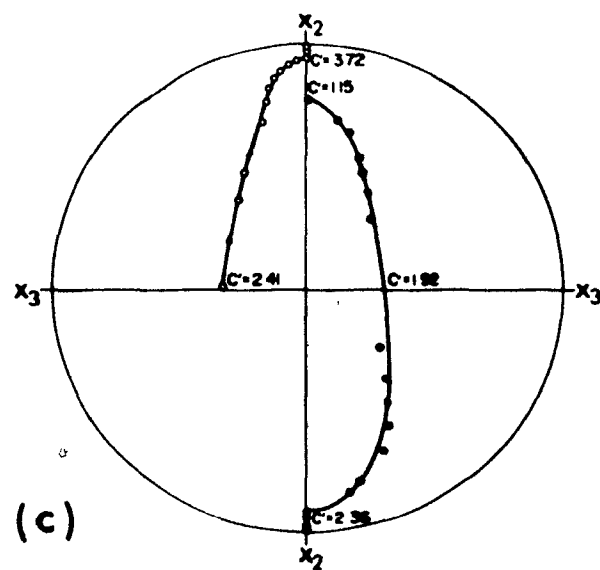
(After Gauthier, Goldsmith and Mason³).



(a)



(b)



(c)

case of rods suspended in viscoelastic media^{2,3)}.

(c) Lateral migration

In addition to the drifts in orbits, rods and discs were found to migrate across the planes of shear in Couette flow towards the region of lower G (in the direction of the outer cylinder) in viscoelastic suspending media, and towards the region of higher G (towards the inner cylinder) in pseudoplastic suspending fluids³⁾.

4. EXPERIMENTAL PART

(a) Apparatus

The suspended particles were observed in the X_2X_3 -plane (Figure 1) in the annulus between two counter-rotating cylinders of a Couette apparatus as described in previous papers from this laboratory^{16,17)} (for details, see Appendix A). The apparatus has a range of shear rates from 0 to 20 sec^{-1} ; most of the experiments here were carried out between 1 and 10 sec^{-1} . The experiments in which an electrical field, applied along the X_2 -axis, were made in an apparatus essentially the same as that above, except the two counter-rotating concentric cylinders were of stainless steel.¹⁶⁾ These were electrically insulated from one another and the electric field applied to the outer cylinder with the inner one grounded. The power supply was 60 Hz a.c. (0 to 25 KV).

The particle rotational motions were recorded

on 16mm cine film using a Paillard Bolex camera aligned with the X_1 -axis. The films were analysed by projecting them onto a drafting table and the changes in particle orientations measured, frame by frame. In order to measure the angle ϕ_1 , the orientation of the reference X_3 -axis was first determined by filming a short sequence of the cylinder wall before each experiment, the angle θ_1 was then calculated from Eqs. [11a] or [11b].

(b) Fluids

The viscoelastic fluids investigated were prepared at a concentration of 2.5% w/V for the aqueous solutions of polyacrylamide, P.A.A. (Cyanamer P. 250, American Cyanamide Company), and up to 5% w/V for polyisobutylene, P.I.B. (Vistanex, Enjay Company, New York, N.Y.) in decahydro-naphthalene (Decalin).

The pseudoplastic media employed were "Close-up" toothpaste, a submicroscopic suspension of silicone in a medium of unknown composition (sample, courtesy of Lever Brothers Inc.) and a neutralised aqueous solution of carboxy-vinyl polymer (Carbopol 940, B.F. Goodrich Chemical Co.) at concentrations up to 0.25 w/V of polymer.

In order to obtain reproducible data, great care had to be taken in the preparation of the polymer solutions, particularly in the case of polyacrylamide where the apparent viscosities were noticeably affected by the stirring rate employed to dissolve them. Such behaviour has been

documented by Haas and MacDonald^{18,19)} who have also given data on the shelf-life of these solutions. All stock solutions of P.A.A. were prepared at the same concentrations employing constant volumes and stirring rates.

(c) Rheological parameters

Various rheological characteristics of the above fluids (except "Close-up" toothpaste) have been reported^{2,3, 20-23)}. In this study, all three normal stress differences and the apparent viscosity were measured at $20^\circ \pm 0.5^\circ\text{C}$ employing the cone and plate fixtures on a Mechanical Spectrometer (Rheometrics Inc., Louisville, Ky.). The cone angle used was 0.04 radians with a plate diameter of 7.2 cm. The elastic moduli were measured on the same instrument utilizing eccentric rotating discs of the same diameter as the cone and plate fixtures. This rotational rheometer has a newly developed transducer system held in place by four cantilever arms each of which supports four piezoresistive silicone cells. This enables an instantaneous and simultaneous measurement of the three separate force components F_1 , F_2 and F_3 acting along the respective coordinates X_1 , X_2 and X_3 (Figure 1a) as well as the resulting torque T_1 . All four results can be displayed on an automatic chart recorder. Here X_1 is the vorticity axis, being the vertical axis of rotation of the spectrometer spindles.

From the above data the shear rate G , the tangential shear stress p_{23} , the apparent viscosity η_0 and

the first normal stress difference ($p_{33} - p_{22}$) (Figure 1b) were calculated by means of the following relationships:

$$\begin{aligned} G &= \omega_1 / \beta \\ p_{23} &= 3T_1 / 2\pi R_c^3 \\ p_{33} - p_{22} &= 2F_1 / \pi R_c^2 \\ \eta_0 &= p_{23} / G \end{aligned}$$

Here ω_1 is the angular velocity of the cone, β the cone angle and R_c the radius of the fixture.

The technique of using eccentric rotating discs for measuring elasticity has been fully described by Macosko²⁴). The geometry of the flow system is shown in Figure 4. The relevant parameters were calculated from the following relationships:

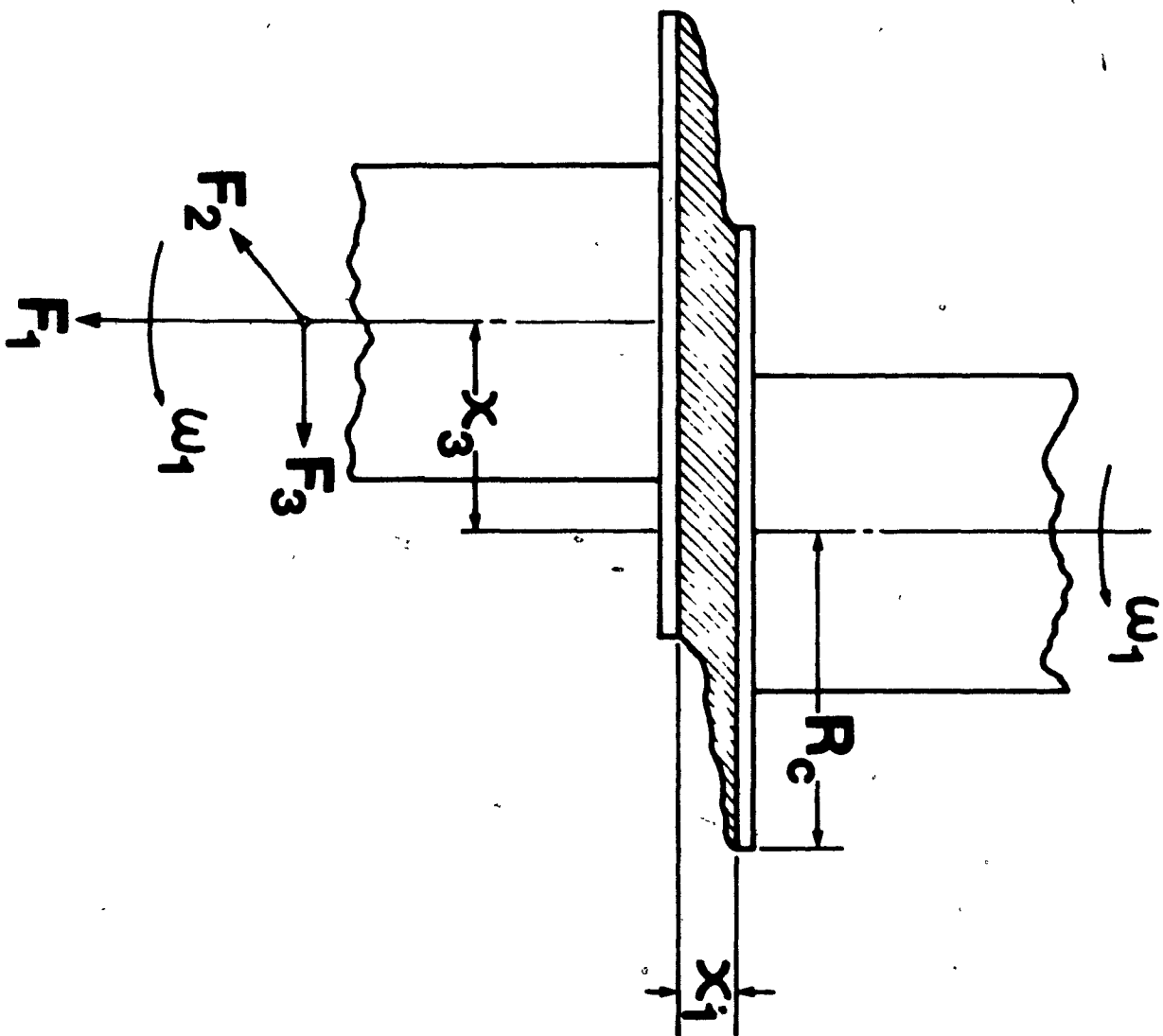
$$\begin{aligned} \text{Strain:} \quad \gamma &= x_3 / x_1 \\ \text{Dynamic shear storage (elastic) modulus} \quad G' &= \frac{F_3 x_1}{\pi R_c^2 x_3} \\ \text{Dynamic shear loss} \quad G'' &= \frac{F_2 x_1}{\pi R_c^2 x_3} \\ \text{Dynamic viscosity} \quad \eta' &= G'' / \omega_1 \end{aligned}$$

Here, x_3 is the horizontal displacement between the axes of the discs (1 mm) and x_1 is the gap width between the parallel plates (also 1 mm).

A decrease in the apparent viscosity with increasing shear rate was found for all the solutions used. This is

FIGURE 4

The geometry of the system for the flow between eccentric rotating discs, where x_3 is the horizontal displacement between disc axes, x_1 the gap width and R_c the radius of the fixture. F_1 , F_2 and F_3 are the forces acting along the respective coordinates x_1 , x_2 and x_3 , when subject to angular velocity ω_1 .



illustrated in Figure 5 over a range of G from 1 to 450 sec^{-1} . The liquids studied were neither rheopectic nor thixotropic.

In addition, as illustrated in Figure 6 both the pseudoplastic and viscoelastic solutions exhibited considerable first normal stress differences, even at shear rates below 1 sec^{-1} . No second or third normal stress differences were detected at the shear rates employed. Although the first normal stress differences increased with increasing shear rates as previously found³⁾, the values of $(p_{33} - p_{22})$ measured in the mechanical spectrometer at a given G were considerably larger, especially in the Carbopol solutions, than those previously obtained using the Weissenberg Rheogeniometer³⁾. A comparison of the results reported by Gauthier³⁾ and those of the present study are shown in Table I. In contrast, the measured apparent viscosities in the present study appear to be in the range previously found by Gauthier³⁾. The discrepancies in the normal stress difference is quite possibly related to the mode of solution which was mentioned earlier.

The storage modulus, the loss modulus as well as the dynamic viscosity are shown in Figure 7 as a log-log plot for angular velocities up to 40 radians sec^{-1} for a polyacrylamide solution and clearly illustrates the presence of considerable elastic modulus. No elastic properties could be ascertained from the test data on the Carbopol solution. Further qualitative evidence for this difference in properties between these two types of fluids was obtained by the presence

FIGURE 5

Apparent viscosity as a function of shear rate rate for "Close-up" toothpaste (closed circles), 0.25% Carbopol solution (closed squares) and 2.5% P.A.A. solution (closed triangles).

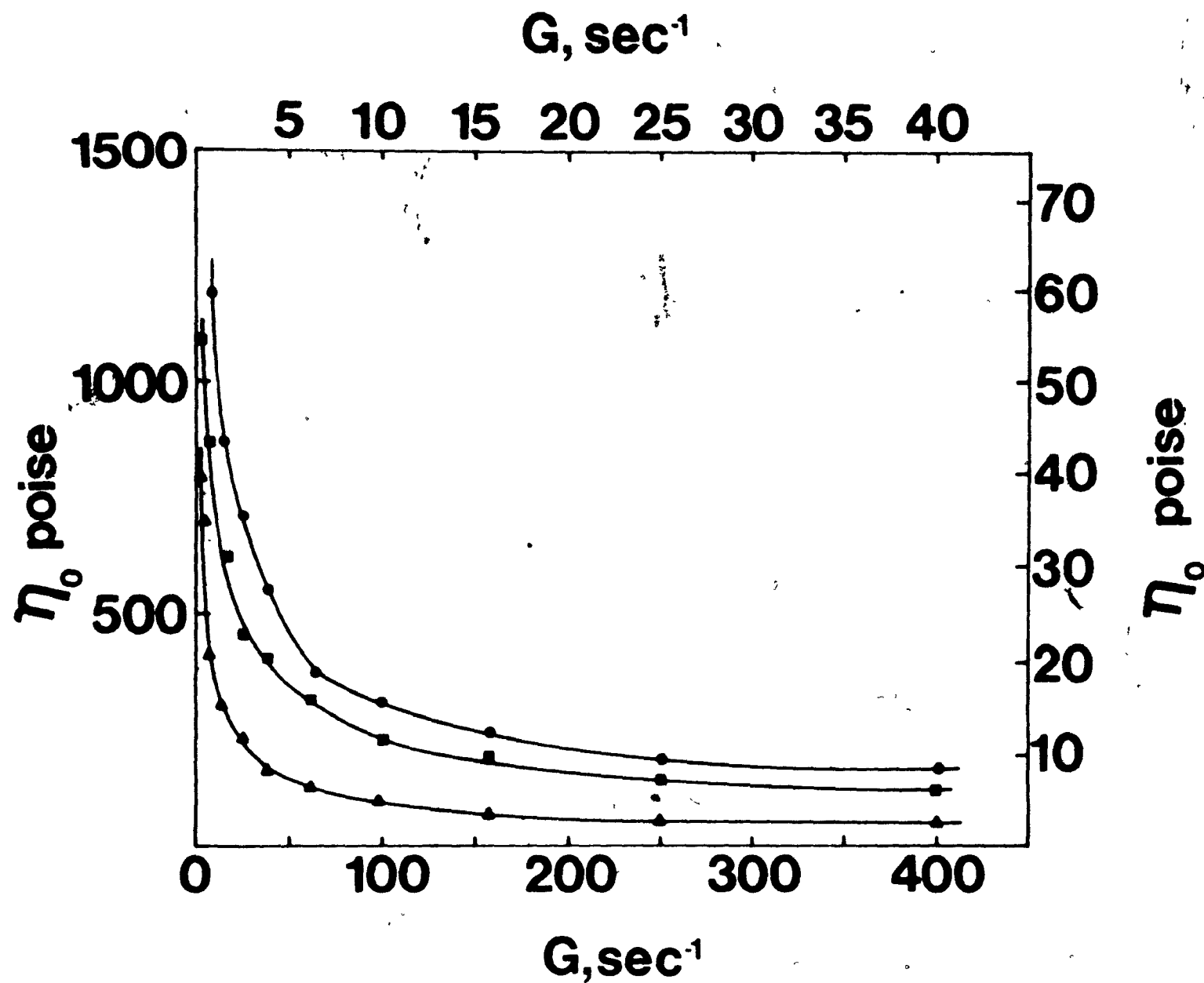


FIGURE 6

Log-log plot of first normal stress
($P_{33} - P_{22}$) against shear rate (sec^{-1})
determined on the Mechanical Spectrometer
using the cone and plate fixtures.

Closed triangles, "Close-up" toothpaste;
closed circles, 2.5% P₄A.A. solution; and
closed squares, 0.25% Carbopol solution.
There were no suspended particles in these
liquids.

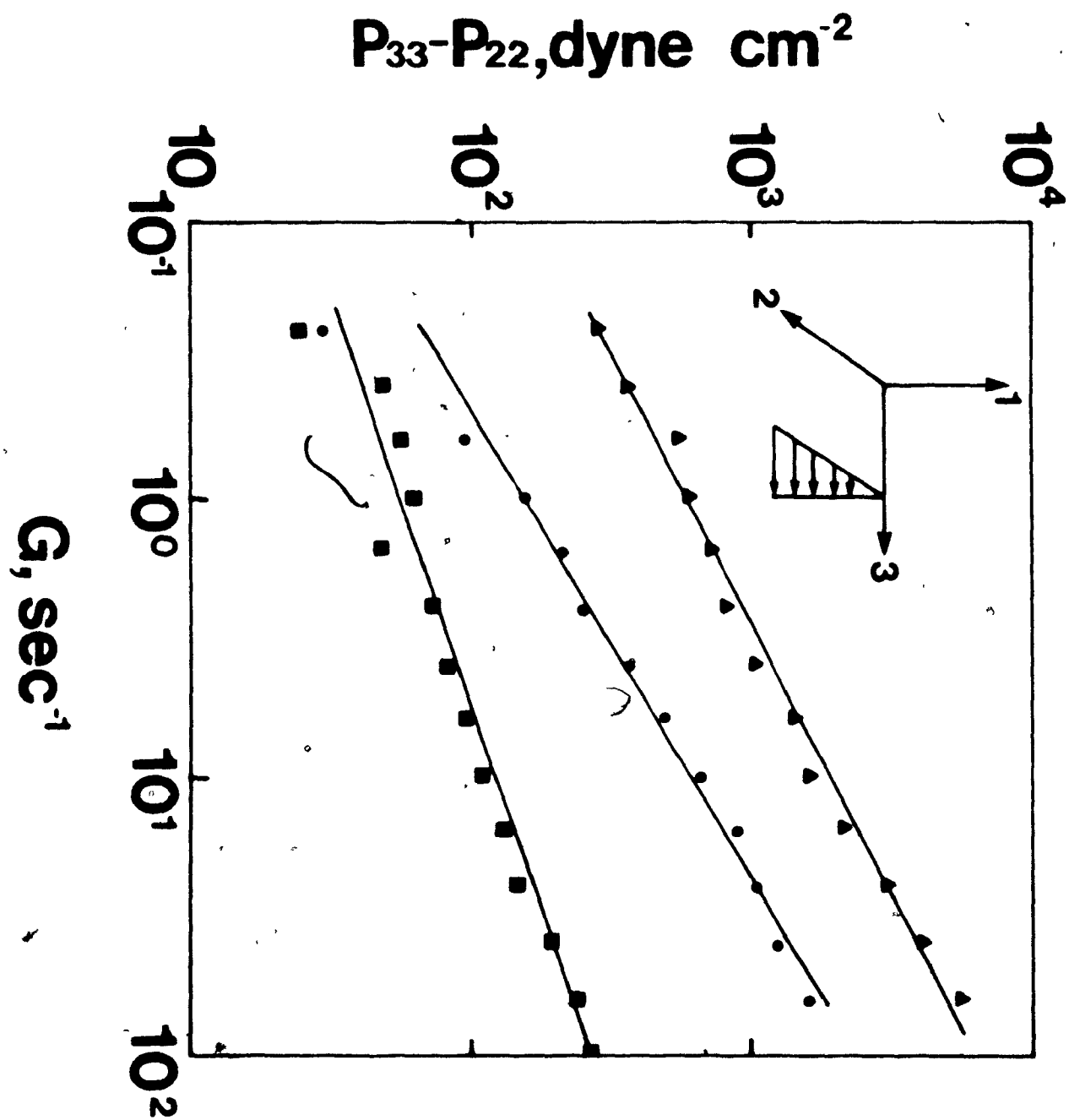


FIGURE 7

Showing a log-log plot of the dynamic viscosity η' , the dynamic shear storage modulus G' and the dynamic shear loss modulus as a function of angular velocity (rad/sec).

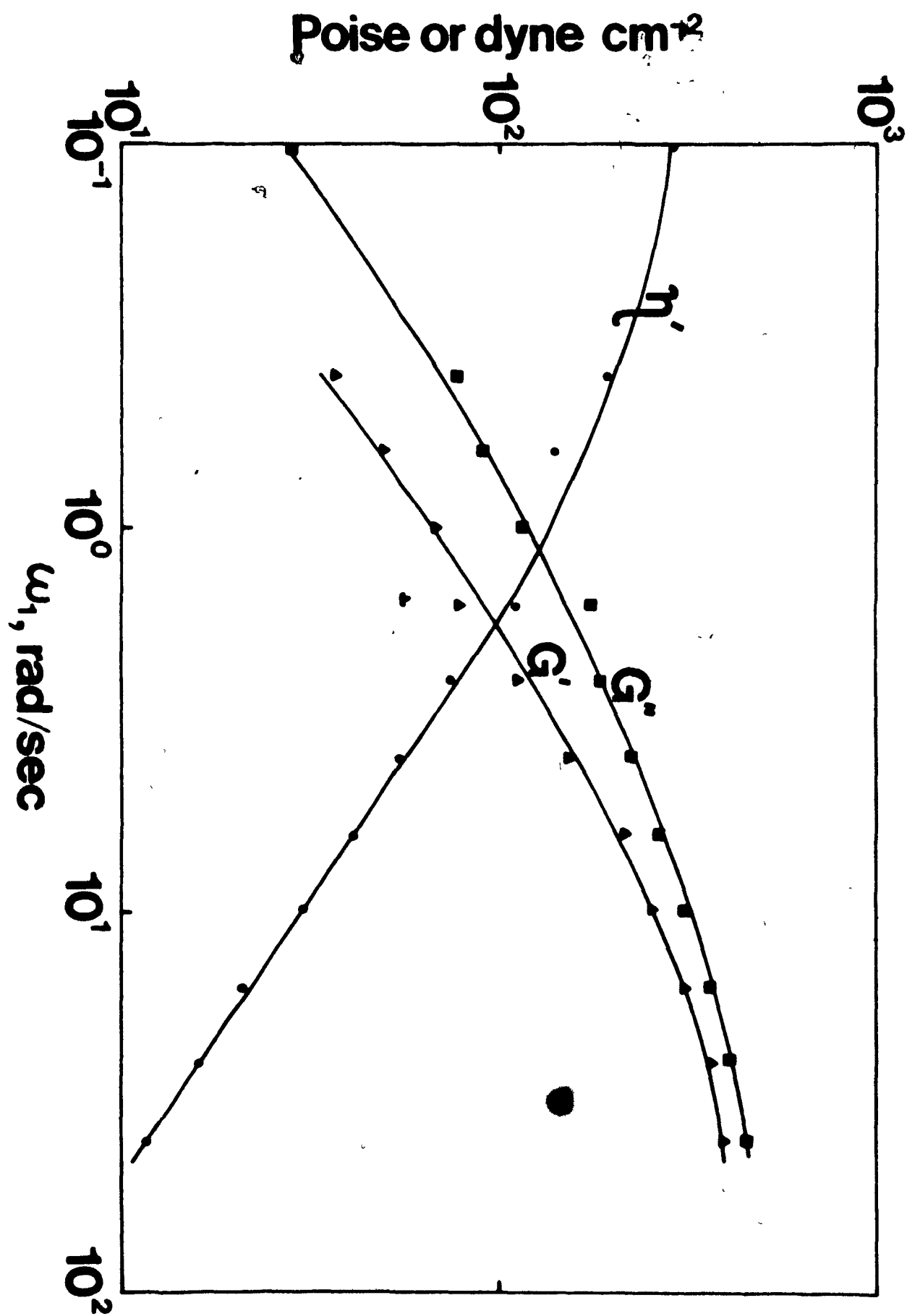


TABLE I

Comparison of first normal stress differences
in fluids; present and previous study ^{a)}

G sec ⁻¹	P ₃₃ - P ₂₂ dyne cm ⁻²				
	GAUTHIER et al.			PRESENT STUDY	
	3% PAA	2% PAA	0.35% Carbopol	2.5% PAA	0.25% Carbopol
1	-	-	0	-	44
5	9	5	0	460	-
10	20	7	0	660	104
100	120	32	~ 0.4	2000	270

a) From Gauthier, Goldsmith and Mason ³⁾.

of the Weissenberg effect upon stirring the viscoelastic solutions and also the translational recovery of small tracer particles in the P.A.A. solution upon cessation of flow. Neither of these effects were observed with the pseudoplastic solutions.

(d) Particles

Discs of diameter 0.180 cm and thickness 0.012 cm were prepared by punching out mylar computer tape. Particles of axis ratios 0.477, 0.675 and 0.881, but constant diameter, were then made by gluing together 7, 10 and 13 discs respectively by placing them in a jig and employing ethyl acetate as the solvent. Examination of the measured particle axis ratios obtained in this manner indicates that some swelling of the mylar occurred during this process. The rods were machine cut from polyethylene filaments of ~ 0.05 cm diameter to give axis ratios of 5.61 and 9.03.

Aluminium coated nylon rods of length 3 mm and diameter 175μ and polyester laminated aluminium discs of diameter 1.83 mm and thickness 94μ were used as the conducting particles in the electrical field experiments, in which a 3% polyisobutylene/decalin solution was used as the suspending medium. Tetrabromoethane was added to this solution to match the densities of the media and the particles.

5. RESULTS

The results described below deal only with particle behaviour in viscoelastic fluids undergoing Couette flow,

since observations made in the pseudoplastic "Close-up" toothpaste and Carbopol solutions at shear rates up to 20 sec^{-1} showed that there was no qualitative difference in the particle motions from those previously found at shear rates $< 5 \text{ sec}^{-1}$. 2,3)

(a) Rotation of discs in 2.5% P.A.A. solutions

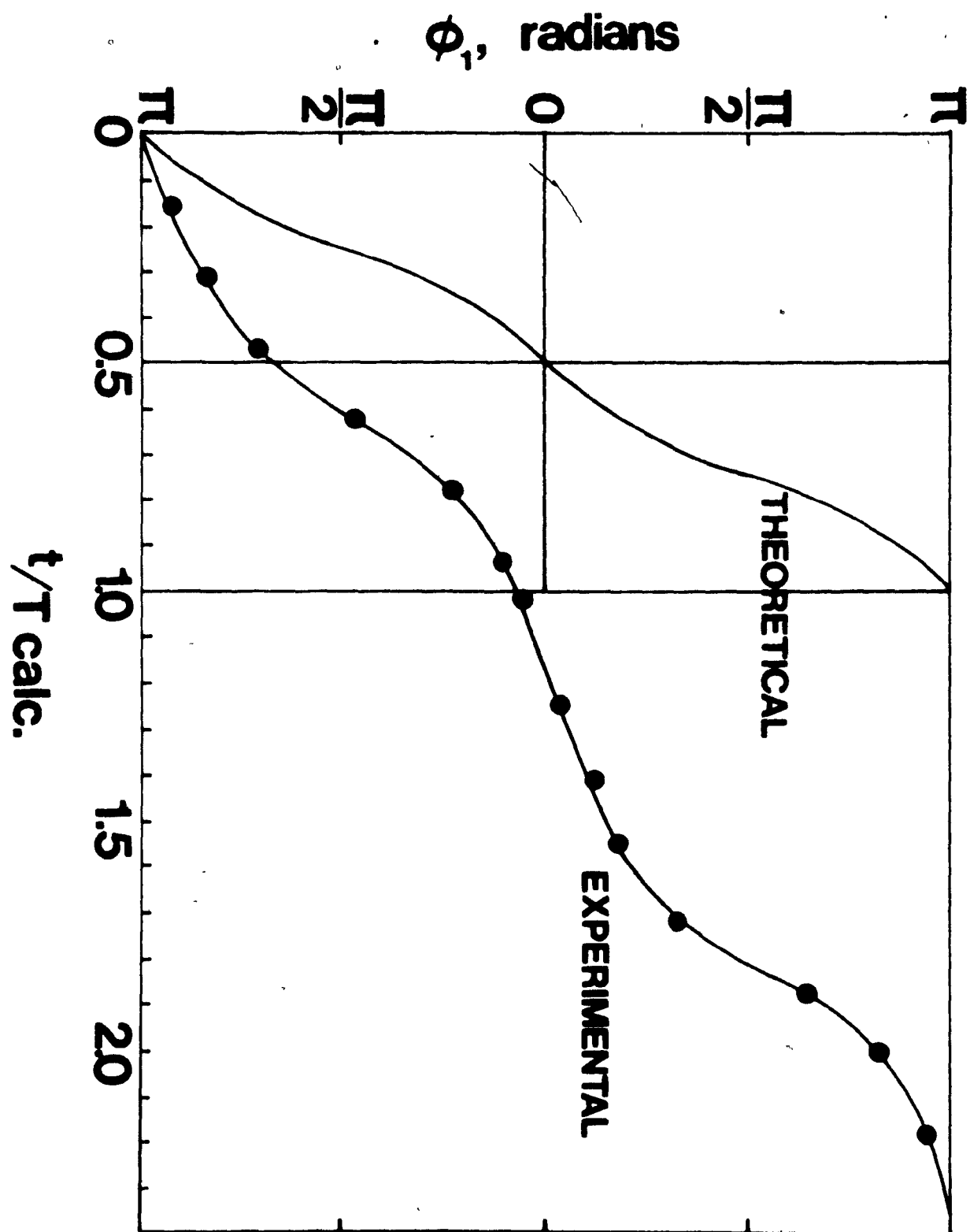
(i) Angular velocities. Unlike previous results obtained for discs of $r_p \sim 0.1$ in this medium³⁾, the observed periods of rotation of particles having axis ratios from 0.067 to 0.881 were markedly greater than those given by theory, as calculated from Eq. [8], with the value of r_e obtained from the measured r_p and Eq. [9]. A comparison of the experimental and ~~calculated~~ values of T for discs of various r_p over a range of G is given in Table 2. In Figure 8, a plot of the measured ϕ_1 against $t/T_{\text{calc.}}$ for a disc ($r_p = 0.477$, $r_e = 0.634$) at a shear rate of 6.53 sec^{-1} , is compared with the theoretical curve calculated from Eq. [7], again using r_e obtained from the empirical relation [9].

It is evident from the table that, at a given r_p , the ratio of the calculated to measured period of rotation increases with increasing shear rate. While there was a marked decrease in $T_{\text{obs.}}/T_{\text{calc.}}$ at $G = 0.15 \text{ sec}^{-1}$ in going from $r_p = 0.067$ to 0.477 a further increase in axis ratio at a given G did not appear to have any significant effect.

(ii) Drift in orbit constant. Again, unlike previous observations in viscoelastic solutions of P.A.A.³⁾ in which

FIGURE 8

Variation of ϕ_1 with time for a rigid disc
 $r_p = 0.477$, $G = 6.53 \text{ sec}^{-1}$. $T_{\text{calc.}}$ is
obtained from Eq. [8] using r_e calculated
from the measured r_p and Eq. [9]. The
theoretical curve is calculated from Eq. [7],
again using r_e obtained from the empirical
relation [9].



thin discs ($r_p = 0.067$) were found to drift into orbits of $C = \infty$, here at low G ($\leq 0.15 \text{ sec}^{-1}$) the discs listed in Table II drifted into equilibrium orbits in which $C < \infty$ and continually varied between a maximum at $\phi_1 = 0, \pi$ and a minimum at $\phi_1 = \pi/2, 3\pi/2$. A portion of such an orbit is shown by a plot of $a'(\phi_1)$ for the disc, $r_p = 0.067$, in Figure 9. Because the period of rotation was almost 500 seconds long, there was appreciable migration of the particle across the planes of shear towards the outer cylinder wall^{2,3)}, taking it out of the field of view of the camera before the complete orbit could be photographed. Similar behaviour was found for discs with axis ratios r_p between 0.477 and 0.881, the particles taking up stable equilibrium orientations with $0 < C < \infty$. Figure 10 shows a typical series of transient orbits for a disc $r_p = 0.675$, as it drifted into an equilibrium orbit. It should be noted that although the particle never rotated in a spherical elliptical orbit with a constant C , the instantaneous values of the orbit constant were computed from Eq. [10] using the measured angles ϕ_1 and θ_1 , and the value of r_e calculated from Eq. [9].

In contrast to the behaviour of thin discs ($r_p < 0.1$) which, as previously observed³⁾, drifted into orbits of $C = \infty$, and at sufficiently high G , aligned themselves with the flow and ceased to rotate (See Figure 3(c)), discs of axis ratios closer to unity continued to rotate in equilibrium orbits in which C was variable and $< \infty$. A comparison of the calculated C values when the axes of revolution were aligned with the X_2 - and

TABLE II

Effect of shear rate and axis ratio on
period of rotation of discs

r_p	r_e ^{a)}	G sec ⁻¹	T sec		$\frac{T_{obs.}}{T_{calc.}}$
			obs.	calc ^{b)}	
0.067	0.141	0.15	490	303	1.62
0.477	0.634	0.15	96.0	93.0	1.04
		1.14	16.4	12.2	1.35
		1.18	16.8	11.8	1.43
		2.44	9.70	5.69	1.70
		3.47	7.32	4.00	1.83
		5.40	5.55	2.57	2.15
		6.53	5.10	2.13	2.40
		8.09	4.20	1.72	2.45
		8.77	4.10	1.58	2.59
		10.6	3.94	1.31	3.02
0.675	0.832	0.15	97.0	85.0	1.14
		1.14	14.8	11.2	1.32
		3.00	5.60	4.26	1.32
		5.40	4.80	2.37	2.03
0.881	0.905	0.15	90.0	84.0	1.07
		1.14	12.9	11.1	1.17
		3.00	5.80	4.21	1.32
		5.40	4.65	2.34	1.99

a) Calculated from Eq. [9] using measured r_p .

b) From Eq. [8] using the measured G and calculated r_e .

FIGURE 9

The equilibrium orbit for a disc,
 $r_p = 0.067$ suspended in 2.5% P.A.A.
solution, $G = 0.15 \text{ sec}^{-1}$, obtained from
the measured projections of the axis of
revolution in the X_2X_3 -plane. The outer
circle corresponds to $C = \infty$.

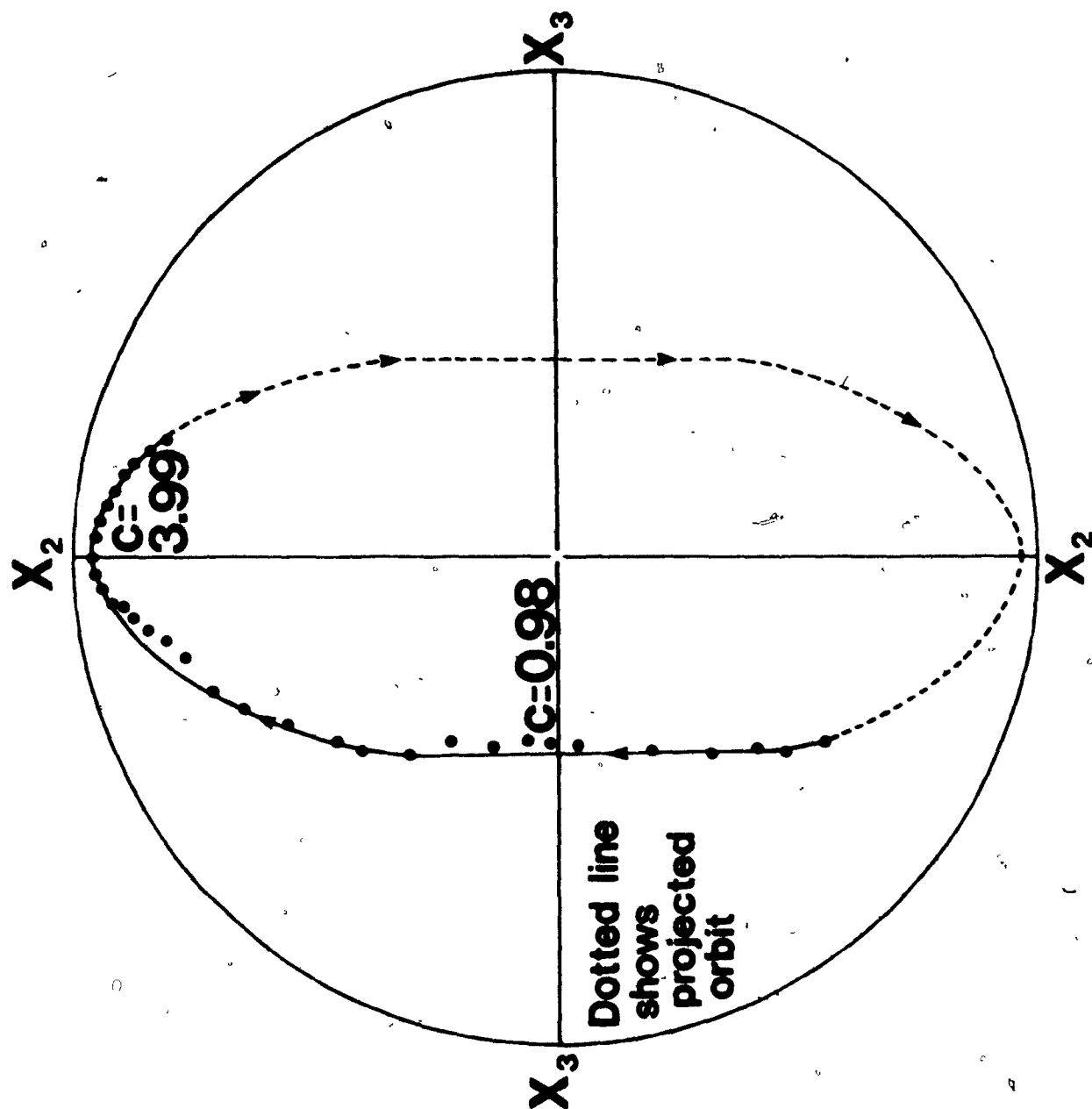
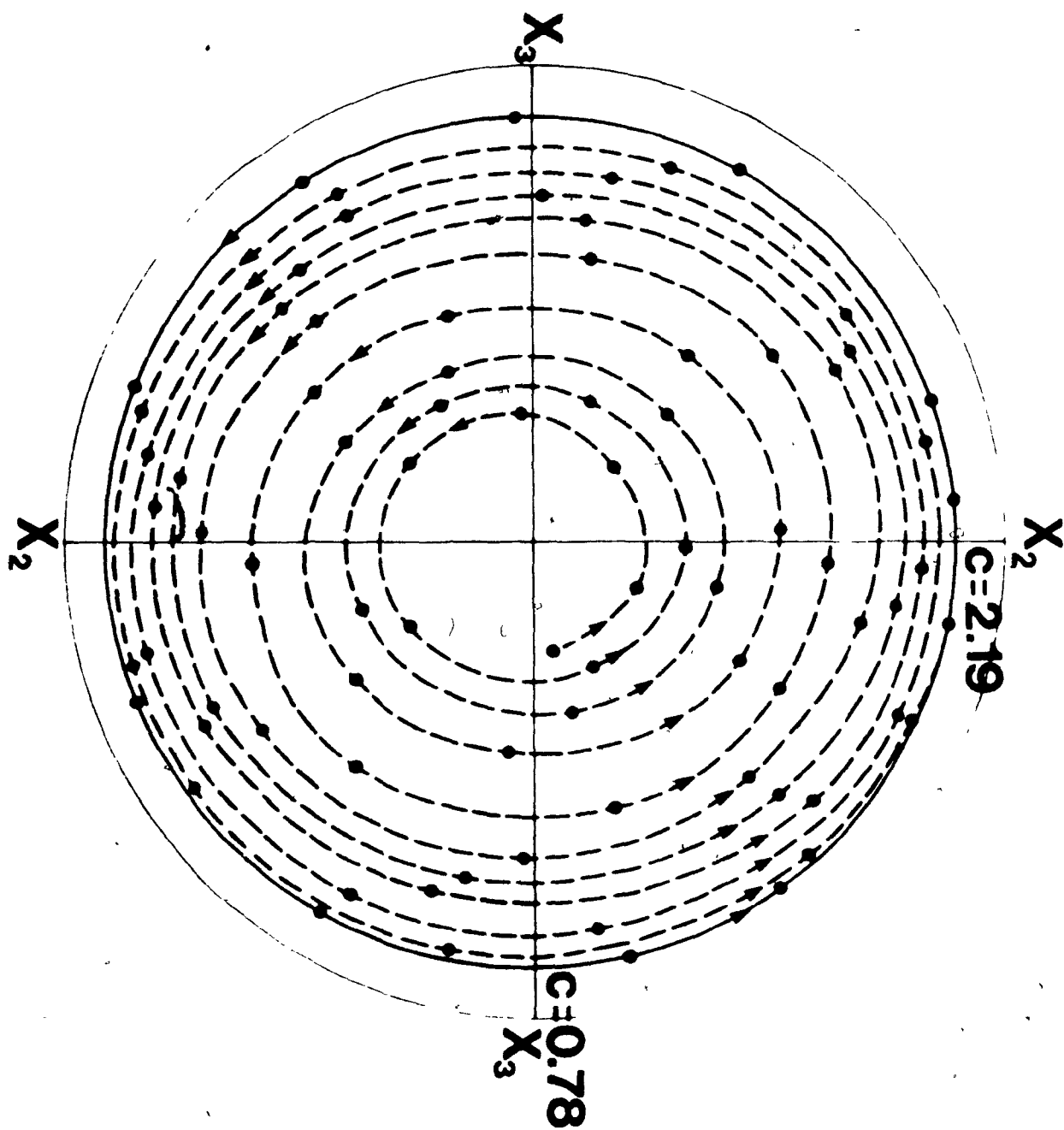


FIGURE 10

Measured projections of one end of the axis of revolution of a disc, $r_p = 0.675$ suspended in 2.5% P.A.A. solution, $G = 1.14 \text{ sec}^{-1}$. The solid line shows the equilibrium orbit and the dotted line the transient orbit constant. The outer circle corresponds to $C = \infty$.



and X_3 -axes is shown in Table III for a series of discs at $G = 5.4 \text{ sec}^{-1}$. The Table shows that as r_e became larger so the equilibrium orbits were characterized by smaller values of the constant C . Projections of the axis of revolution for discs with $r_p = 0.477, 0.675$ and 0.881 at $G = 1.14 \text{ sec}^{-1}$ are shown in Figure 11. The effect of increasing shear rate on the equilibrium orbit of a given disc is shown in Figure 12, where it may be seen that the value of C at $\phi_1 = \pi/2$ decreases while that at $\phi_1 = 0$ remains sensibly constant. Table IV lists the values of C at $\phi_1 = 0$ and $\pi/2$ at shear rates from 1.14 to 10.6 sec^{-1} for a disc, $r_p = 0.881$.

(b) Rotation of rods in viscoelastic media

The gradual, steady drift in orbit of rods to an orientation where the major axis is aligned with the vorticity axis, $C = 0^{2,3)}$ was again observed in this study at shear rates $< 0 \text{ sec}^{-1}$ both in pseudoplastic solutions of Carbopol and "Close-up" Toothpaste, as well as in the viscoelastic solutions of P.I.B. and P.A.A. (see Figure 3b). However, at higher shear rates in the viscoelastic media a behaviour analogous to that of the non-rotating disc aligned with the direction of flow was found. This occurred when a rod was initially aligned with the X_2 -axis and lay in, or very close to, the X_2X_3 -plane. Upon shearing the fluid, the particle rotated to the orientation $\phi_1 = \pi/2$ and then, once aligned with the flow, ceased to rotate. This was observed

46

FIGURE 11

Showing equilibrium orbits for discs of
various axis ratios suspended in 2.5%
P.A.A. solution subjected to a shear rate
of $G = 1.14 \text{ sec}^{-1}$.

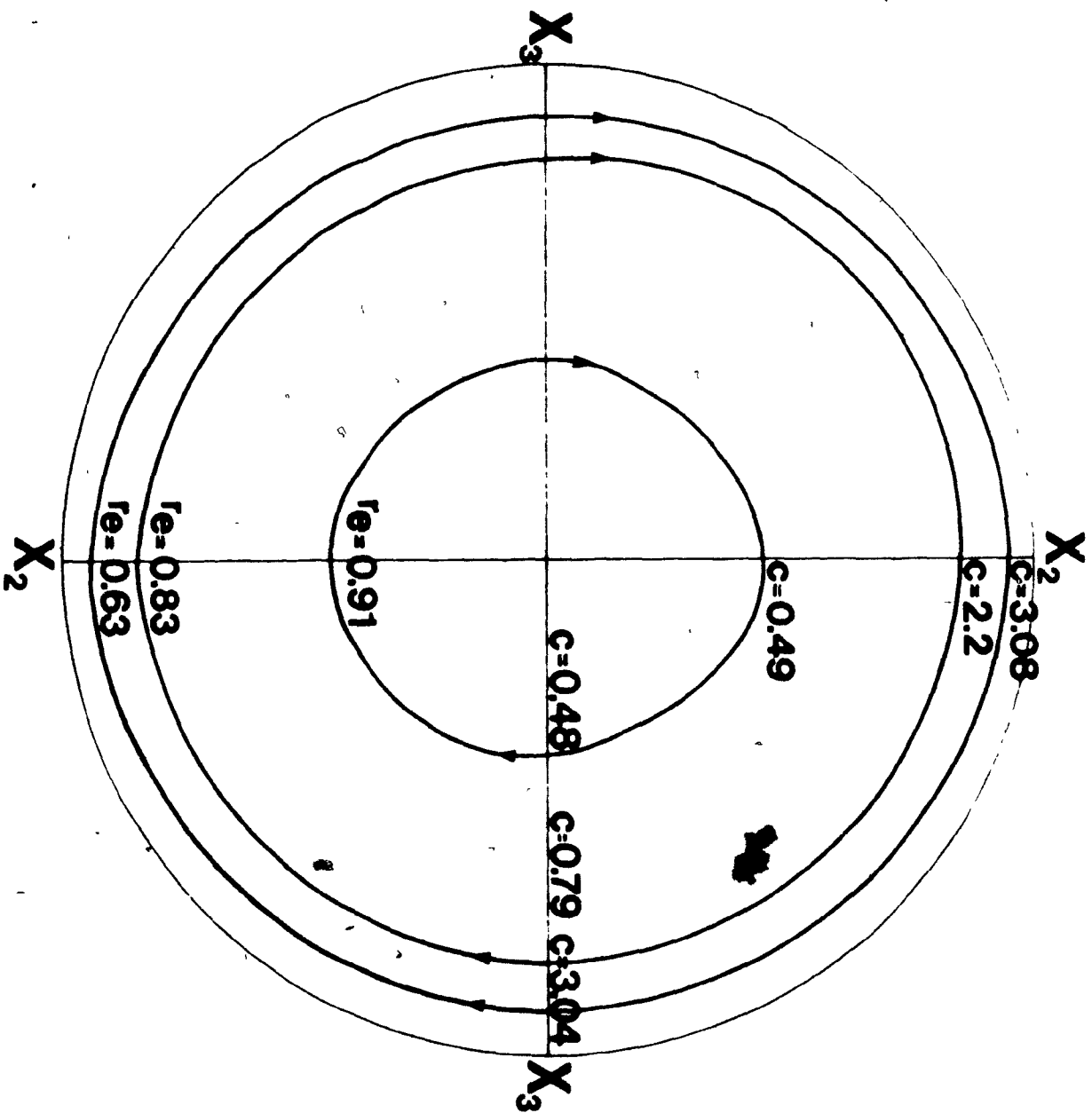


TABLE III

Equilibrium orbit constants at $\phi_1 = 0$ and
 $\pi/2$ as a function of axis ratio

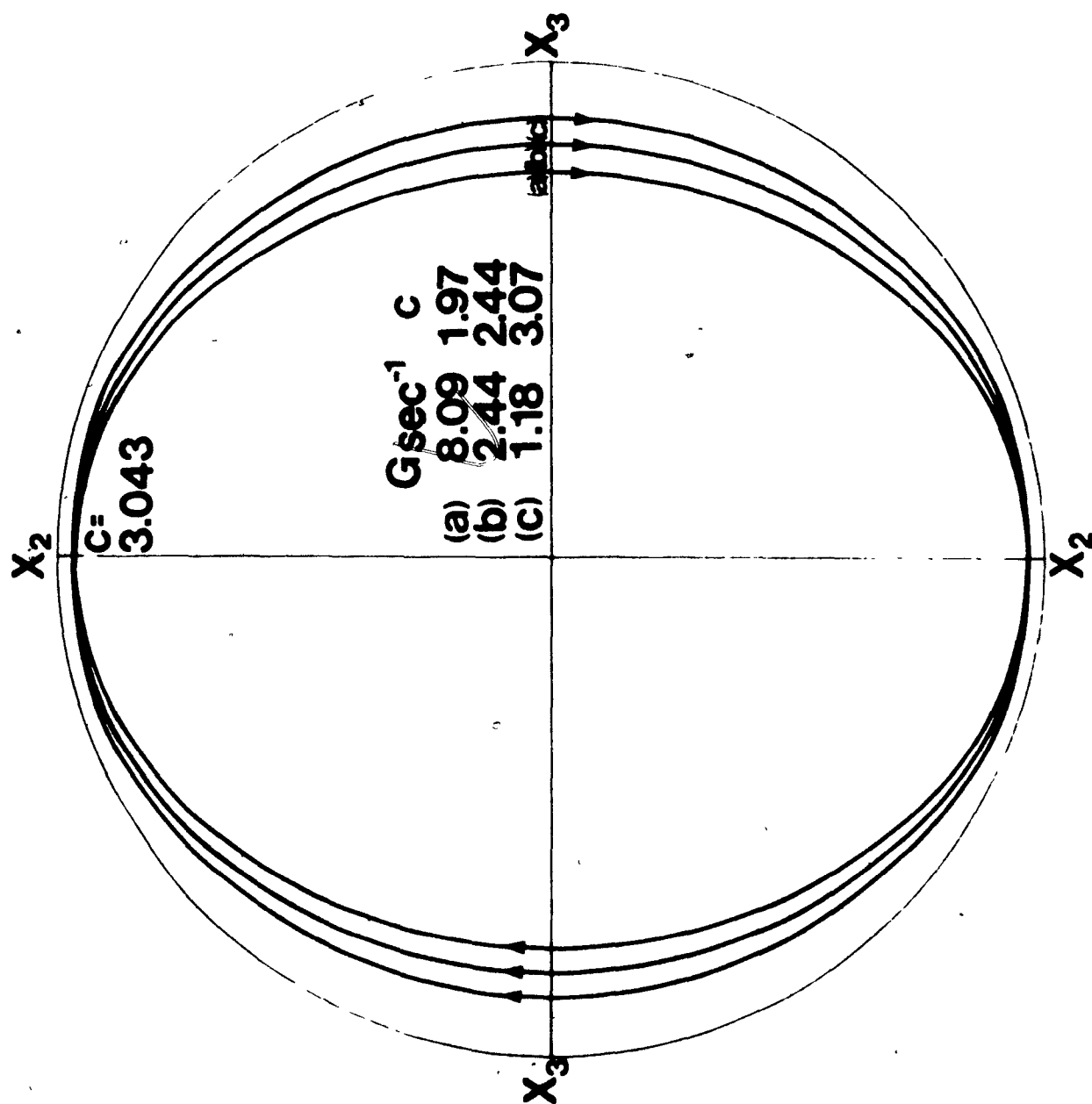
2.5% PAA Solution
 $G = 5.4 \text{ sec}^{-1}$

r_p	r_e	Orbit constant C ^{a)}	
		$\phi_1 = 0$	$\phi_1 = \pi/2$
0.067	0.141	∞	∞
		non-rotating particle	
0.477	0.634	2.53	2.10
0.675	0.832	2.35	1.66
0.881	0.905	1.32	1.08

a) Calculated from Eq. [10], with r_e
calculated from Eq. [9].

FIGURE 12

Equilibrium orbits for a discs, $r_e = 0.634^\circ$
suspended in 2.5% P.A.A. solution at various
shear rates. The outer circle corresponds
to $C = \infty$.



v

TABLE IV

Equilibrium orbit constants for a
disc as function of shear rate

$r_p = 0.881$
2.5% PAA solution

G sec ⁻¹	T _{obs.} sec.	Orbit Constant		Ratio
		$\phi_1 = 0$	$\phi_1 = \pi/2$	
1.14	16.8	3.04	3.08	0.99
2.44	9.7	3.04	2.44	1.25
3.47	7.3	3.43	2.78	1.23
6.53	5.1	2.35	1.79	1.31
8.09	4.2	3.04	1.97	1.55
8.77	4.1	3.04	1.97	1.55
10.6	/ 3.8	3.04	1.79	1.70

with rods of axis ratio 9.03, suspended in 2.5% P.A.A. at $G > 5 \text{ sec}^{-1}$. The rods remained in this orientation provided that there were no particle interactions or disturbances to the flow. If these occurred, the particles resumed their angular motion and drifted into the orbit $C = 0$.

A variation of the above described motions was found for rods of shorter r_p , which again if initially placed in the orientation $\phi_1 = 0$ and lying in the X_2X_3 -plane exhibited the following four stages of behaviour:

(i) The rod rotated through the first quadrant of its orbit with only small changes in orbit constant, then when aligned with the X_3 -axis,

(ii) there was no further change in ϕ_1 or θ_1 -orientation for a period as long as 10 sec and during this "residence" time the rod migrated slowly towards the outer cylinder wall.

(iii) After the "residence time" there followed a shorter "induction period" during which the angle θ_1 increased without a change in the angle ϕ_1 . This continued until the rod reached a critical θ_1 -orientation, whereupon,

(iv) the angular rotation of the rod resumed and the particle drifted through a series of transient orbits to a final orientation $C = 0$. An X_2X_3 -projection of the axis of revolution during this process is shown in Figure 13. The time course of the above events is illustrated in Figure 14 by plots of ϕ_1 and $\sin\theta_1$.

FIGURE 13

Measured projections of one end of a rod
 $r_p = 5.6$ suspended in 2.5% P.A.A. solution
($G = 6.43 \text{ sec}^{-1}$) showing the different
stages of behaviour in the progressive
drift of the orbit constant from C' close
to ∞ to C' close to 0 in the direction
given by the arrows.

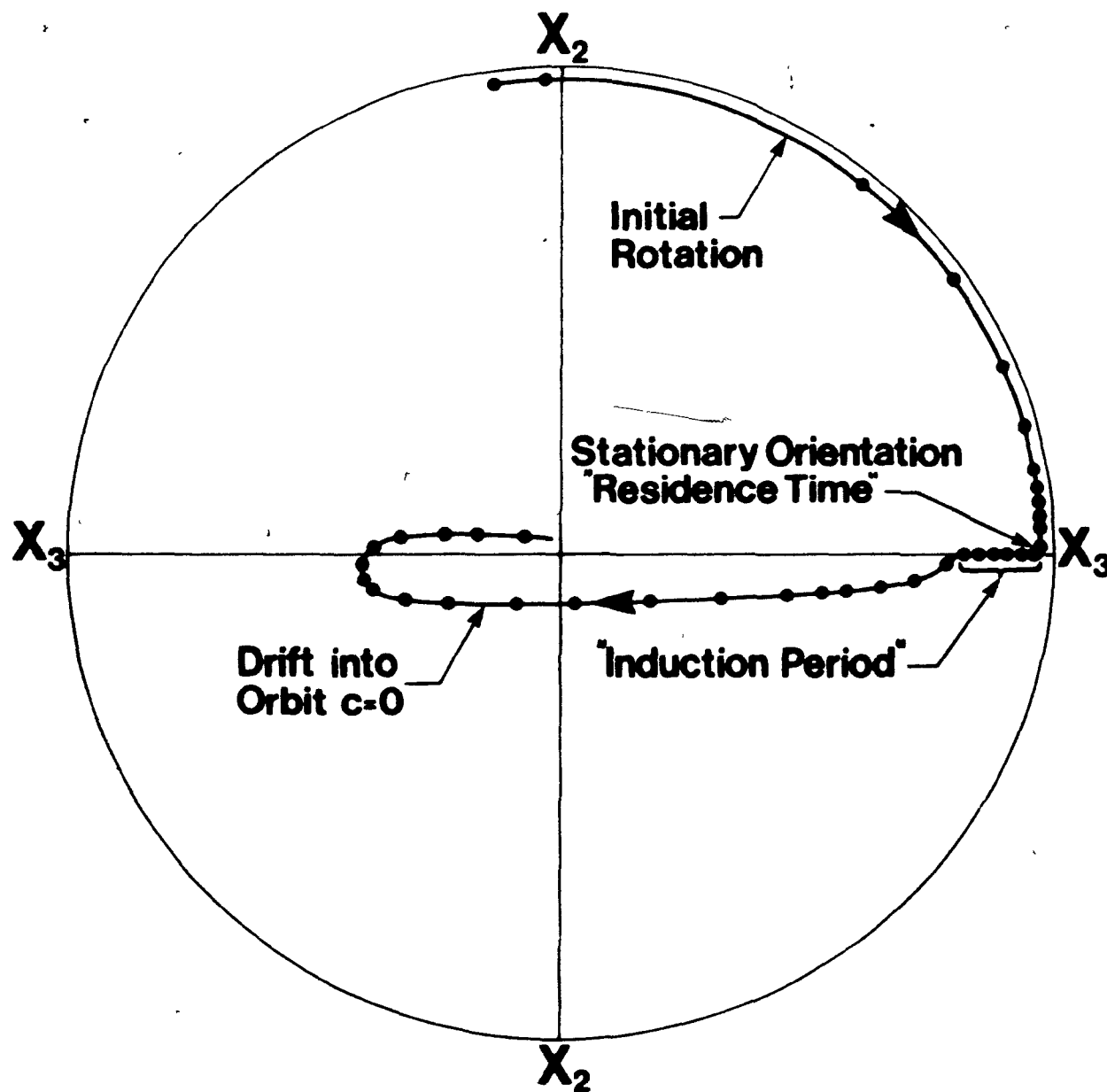
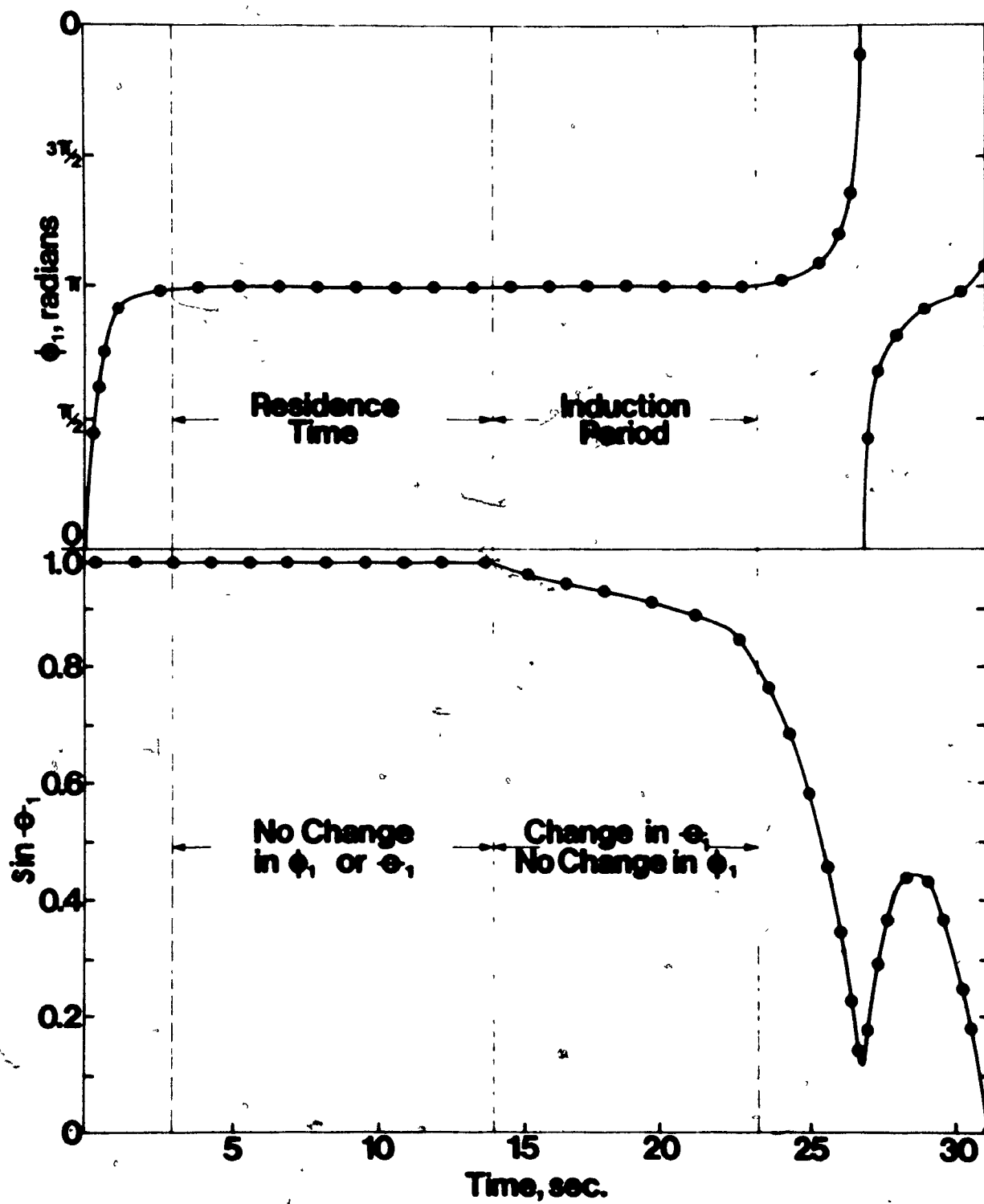


FIGURE 14

Showing the variation of ϕ_1 and $\sin\theta_1$ with time for a rod suspended in a viscoelastic liquid. Same particle and conditions as in Figure 13.



c) Rotation of rods and discs in shear and electric fields in 3% polyisobutylene/decalin solution

Single, isolated conducting rods ($r_p = 17.14$) and discs ($r_p^1 = 0.052$) in shear flow were allowed to reach the equilibrium orbits of $C = 0$ and $C = \infty$ respectively (no experiments were carried out with the rod in the non-rotating equilibrium position with $C = \infty$). An A.C. electric field of ~ 1000 volts was then applied across the annular gap and the following observations of particle behaviour noted. Both discs (whether non-rotating or rotating) and rods left their limiting orbits and drifted into equilibrium orbits in which $0 < C < \infty$. A further increase in the magnitude of the electric field resulted in a further change in equilibrium orbit. However, when the electric field was removed, the original limiting orbits were regained. Similar behaviour has been observed²⁵⁾ for these particles in a 0.25% pseudoplastic solution of Carbopol/propylene glycol.

6. CONCLUDING REMARKS

A previous study³⁾ with rods and discs in pseudoplastic Carbopol solutions had shown that the experimentally determined period of rotation and that calculated from Eq.[8] were in good agreement and that this was also true for viscoelastic fluids of P.A.A. at low shear rates. However, the present investigation has demonstrated that even at relatively low shear rates in 2.5% P.A.A. solution there is a pronounced

increase in the period of rotation from that predicted using Jeffery's theory, and that this difference further increases with increasing shear rate. No doubt such discrepancies in observed and measured angular velocities (cf. Figure 8) are due to an elastic restoring torque, which at low G results in the retardation of the angular velocity and thus an increase in the period of rotation. Eventually, as previously observed³⁾ when the velocity gradient reaches a critical value, rotation ceases and the disc aligns itself with the flow. Now, as previously stated by Gauthier³⁾ "The alignment ... is most likely due to the elastic properties of the polyacrylamide solutions which increase with increasing polymer concentration and which, during shear give rise to a restoring torque opposing that due to viscous deformation of the fluid. When the particles cease to rotate, the two torques balance each other ... As G is further increased, the particle remains at a constant orientation indicating that the elastic torque is increasing faster than the hydrodynamic torque". The fact that the above phenomenon does not occur in pseudoplastic solutions of Carbopol can then be attributed to the absence of an elastic modulus in these fluids.

In the present work, for the first time a similar phenomenon was observed with rods, although here the equilibrium position of alignment with the flow in which the particle lies in the X_2X_3 -plane is a metastable one.

The fact that some of these phenomena were not previously observed may in part be a reflection on the much

higher normal stresses and, one presumes, elastic moduli of the P.A.A. solutions used in the present work.

The observations that the drift into limiting rotational orbits of minimum energy dissipation in the flow occurs both in pseudoplastic and viscoelastic polymer solutions^{2,3)} suggests that it is the first normal stress difference which is responsible, and that the modifications of the above behaviour observed with discs of the same diameter but with r_p closer to unity suspended in P.A.A. solutions are due to the presence of the elastic properties of the fluid. Thus for discs in 2.5% P.A.A. solution at a given shear rate, as the r_p value increased from 0.067 to 0.881, the equilibrium orbit decreased from $C = \infty$ to C close to unity. For particle axis ratios above unity, the first normal stress difference and the elastic modulus appear to complement each other in the steady drift in the orbit towards the asymptotic value of $C = 0$.

Nevertheless, in the absence of theory giving quantitative descriptions of the rheological properties of these non-Newtonian fluids, the above considerations must be considered speculative.

LIST OF SYMBOLS

$2a; 2a'(\phi_1)$	= axis of revolution of spheroids; projection of this axis on the X_2X_3 -plane at ϕ_1 .
$b; b'(\phi_1)$	= equatorial diameter; and projection of this axis on the X_2X_3 -plane at ϕ_1 .
c	= orbit constant.
E	= electric field.
F_1, F_2, F_3	= normal forces measured along the X_1, X_2, X_3 axes of a mechanical spectrometer.
$G; G(R)$	= velocity gradient, at R in the Couette annulus.
$G'; G''$	= dynamic shear storage modulus; dynamic shear loss modulus.
K, n	= constants for power law fluid.
$P_{23}; P_{33} - P_{22}$	= tangential shear stress; first normal stress difference.
r_p	= particle axis ratio = a/b .
r_e	= equivalent ellipsoidal axis ratio
$R; R_I, R_{II}$	= radial distance of the particle centre from the axis of rotation in Couette flow; radius of inner and outer cylinders of Couette apparatus.
R_c	= radius of the fixtures of the mechanical spectrometer.
R_{23}	= axis ratio of the ellipse, projection of particle rotational orbit in the X_2X_3 -plane.
t	= time
$T,$	= period of rotation of particle
T_1	= total torque applied on liquid in mechanical spectrometer.
u_3	= fluid velocity along X_3 -axis.

x_1, x_2, x_3 = Cartesian coordinate axes of the external flow field.

x_1, x_3 = distance between the plates and axial displacement of eccentric rotating discs.

Greek

β = cone angle

η_0, η' = apparent viscosity, dynamic viscosity.

γ = strain

θ_1, ϕ_1 = spherical polar coordinates referred to the polar axis x_1 of the external flow field.

ω_1 = angular velocity of spheroid or mechanical spectrometer fixtures.

$\Omega(R); \Omega_I, \Omega_{II}$ = angular velocity of the fluid at R ; angular velocities of the inner and outer cylinders of the Couette apparatus.

REFERENCES

1. Goldsmith, H.L. and Mason, S.G., in *Rheology: Theory and Application* (F.R. Eirich, ed.), Vol. 4, Chapter 2, 85-250, Academic Press, New York, (1967).
2. Karnis, A. and Mason, S.G., *Trans. Soc. Rheol.* 10, 571 (1967).
3. Gauthier, F., Goldsmith, H.L. and Mason, S.G., *Rheol. Acta*, 10, 344 (1971).
4. Jeffery, G.B., *Proc. Roy. Soc. (London)*, A102, 161 (1922).
5. Brenner, H., *Advances in Chem. Eng.* 6, 287 (1965).
6. Taylor, G.I., *Proc. Roy. Soc. (London)*, A138, 41 (1932).
7. Einstein, A., "Eine neue Bestimmung der Molekuldimensionen", *Ann. de Physik*, 19, 289 (1906); with a correction in 34, 591 (1911).
8. Oberbeck, "Crelle", vol. 81 (1876).
9. Edwards, 'Quart. Jour. Math.', vol. 26 (1892).
10. Trevelyan, B.J. and Mason, S.G., *J. Colloid Sci.*, 6, 354 (1951).
11. Okagawa, A. and Mason, S.G., *J. Colloid Interface Sci.* (in press, 1973).
12. Goldsmith, H.L. and Mason, S.G., *J. Fluid Mech.* 12, 88 (1962).
13. Anczurowski, E. and Mason, S.G., *J. Colloid Interface Sci.* 23, 583 (1967).
14. Goldsmith, H.L. and Mason, S.G. *J. Colloid Sci.* 17, 448 (1962).
15. Darabaner, C.L. and Mason, S.G., *Rheol. Acta*, 6, 273 (1967).
16. Bartok, W. and Mason, S.G., *J. Colloid Sci.* 12, 243 (1957).
17. Darabaner, C.L., Raasch, J.K. and Mason, S.G., *Can. J. Chem. Eng.* 45, 3 (1967).
18. Haas, M.C. and MacDonald, R.L., *Polymer Letters* 10, 461 (1972).

19. Haas, M.C. and MacDonald, R.L., J. App. Poly. Sci. 16, 2709 (1972).
20. Greensmith, M.W. and Rivlin, R.S., Nature 186, 664 (1951).
21. Greensmith, M.W. and Rivlin, R.S., Trans. Roy. Soc. (London), A245, 399 (1953).
22. Philippoff, W., Trans. Soc. Rheol. 1, 95 (1957).
23. Brodnyan, J.G., Gaskins, F.M. and Philippoff, W., Trans. Soc. Rheol. 1, 109 (1957).
24. Macosko, C., "Flow of Polymer Melts between Eccentric Rotating Discs", Polymer Materials Program, Dept. of Chem. Eng., Princeton Univ., Princeton, N.J.
25. Gauthier, F. (unpublished).

PART III

BEHAVIOUR OF DEFORMABLE PARTICLES IN NEWTONIAN
AND NON-NEWTONIAN LIQUIDS, HAVING ZERO OR
NEAR ZERO INTERFACIAL TENSION

1. ABSTRACT

A preliminary study of the behaviour of deformable particles undergoing slow Couette flow was undertaken, where the drop and the medium were mutually soluble. For Newtonian systems a fair agreement with theory was observed. Thus, when the drop was much more viscous than the medium, the deformation parameter D' , and the transient orientation α' , oscillated without damping, whereas for the drop/medium viscosity ratio $\lambda < 1$, D' and α' were found to increase steadily with time to asymptotic values of 1.00 and 90° respectively. This latter case was also observed for viscoelastic systems when $\lambda < 1$. However, for viscoelastic pairs when $\lambda \gg 1$, the drop deformed into a cylinder with its long axis aligned along the vorticity axis and the subsequent break-up formed two or more daughter cylinders. This phenomenon was repeated until the two liquids were completely indistinguishable. Results indicated that this behaviour was a consequence of both the elastic properties of the system and the zero interfacial tension. Pseudoplastic drops in viscoelastic fluids were found to follow the class A mode of deformation up to burst.

2. INTRODUCTION

This investigation was undertaken to extend earlier experimental¹⁻⁵⁾ and theoretical⁶⁾ studies from this laboratory dealing with the behaviour of fluid drops in shear flow. In particular, to verify experimentally, a part of the most recent theory⁶⁾ concerning the deformation and orientation of Newtonian fluid systems with zero interfacial tension. Also, due to the scarcity of literature, either theoretically or experimentally, concerning the dispersion of drops in totally non-Newtonian systems (in most cases at least one of the liquid phases was Newtonian) included in the present study are the results of the behaviour of pseudoplastic and viscoelastic drops suspended in viscoelastic media.

3. THEORETICAL AND EXPERIMENTAL BACKGROUND

a) Deformation and orientation of drops

The case of a liquid drop of radius b and viscosity η_1 immersed in a second immiscible fluid of viscosity η_2 undergoing Couette flow as shown in Figure 1, $u_1 = 0$, $u_2 = 0$, $u_3 = GX_2$, G being the velocity gradient, was first treated by Taylor^{7,8)}. He obtained the result that deformation of the drop from its initial spherical shape depends only upon two dimensionless parameters $\lambda = \eta_1/\eta_2$ and $k = Gb \eta_2/\sigma_{12}$, where σ_{12} is the interfacial tension of the 12 interface⁸⁾. For two particular cases in steady shear flow, Taylor showed that the drop deforms into an ellipsoid whose axes are


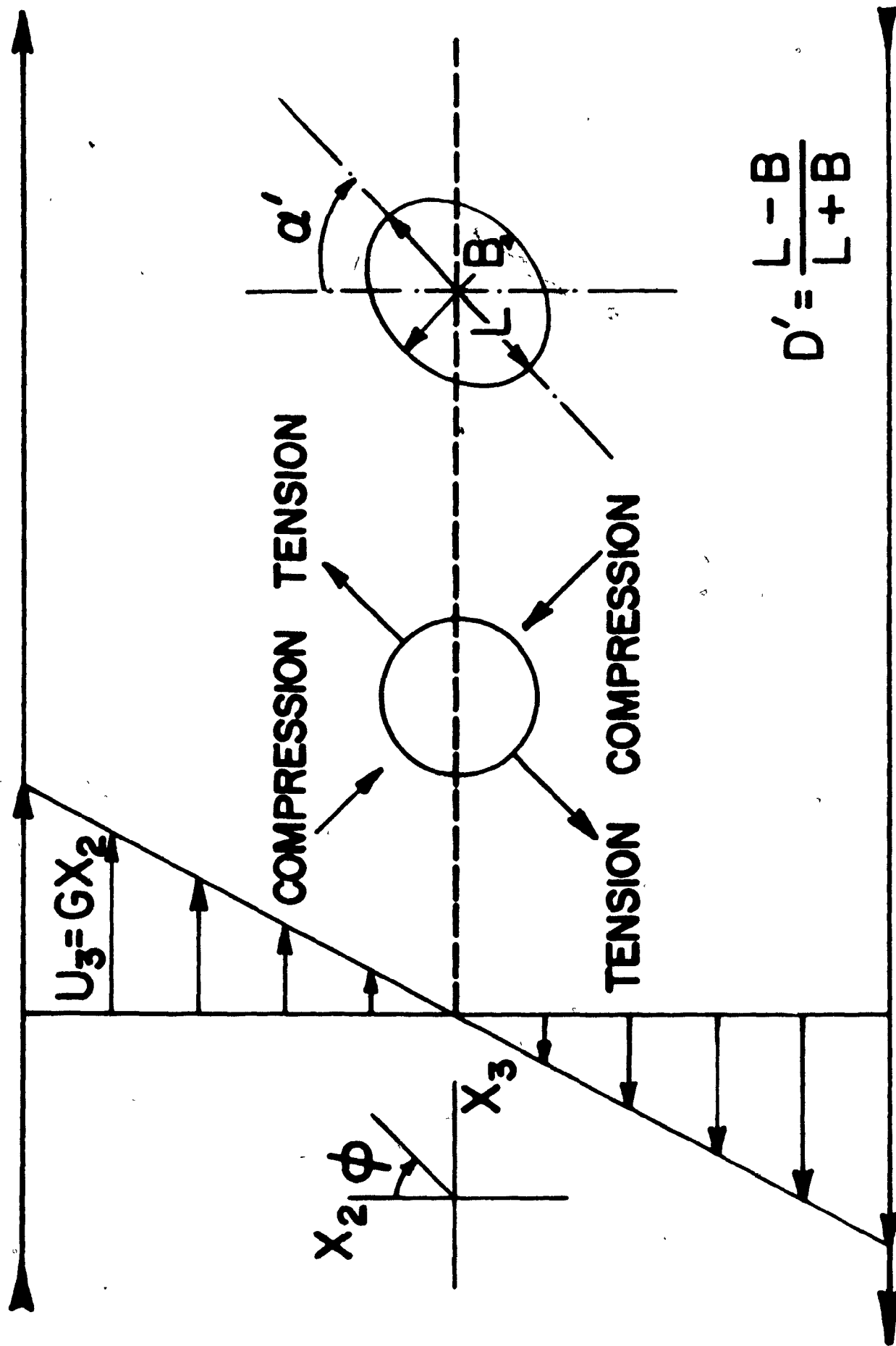


Figure 1 Cartesian (X_1, X_2, X_3) and spherical polar coordinates (r, ϕ, θ) for the shear flow; X_1 and θ are not drawn. The principal axes of deformation are indicated by the arrows on the undeformed drop. The transient deformation parameter D' , which is always positive, and the transient orientation angle α' of the deformed drop are indicated on the right. The centre of the drop lies in the stationary layer where $U_3 = 0$. (After Torza, Cox and Mason)



$$D' = \frac{L - B}{L + B}$$

$2b(1+D)$, $2b$, and $2b(1-D)$, of which the first and third correspond to the length L and breadth B of the respective major and minor axes (Figure 1), the particle being oriented at an angle α to the X_2 - axis of the flow field:

case (i)

λ fixed, $k \rightarrow 0$

$$\alpha \approx \pi/4; D = k \left(\frac{19\lambda + 16}{16\lambda + 16} \right). \quad [1]$$

case (ii) $\lambda \rightarrow \infty$, k fixed

$$\alpha = \pi/2; D = 5/4\lambda. \quad [2]$$

D is a steady deformation parameter, physically given by

$$D = \frac{L - B}{L + B} \quad [3]$$

Equations [1] and [2], which were derived under conditions that D is close to zero, have been shown to apply in various systems undergoing Couette flow¹⁻³⁾.

Subsequent theoretical studies of drop deformation^{3,9-11)}, while providing a more accurate expression for the orientation α at low λ , essentially treated the problem in the manner of Taylor. Recently, however, Cox⁶⁾ has given a more general theory for the time dependent deformation D' of a drop which places no limitations on k or λ and is subject only to the condition that $D' \rightarrow 0$. The time dependent deformation D' and orientation α' of a spherical drop initially placed in a fluid at rest was shown to be given by

$$D' = D \left[1 - 2e^{-\frac{20Gt}{19k\lambda}} \cos(Gt) + e^{-\frac{40Gt}{19k\lambda}} \right]^{1/2} \quad [4a]$$

$$\alpha' = \frac{\pi}{4} - \frac{1}{2} \tan^{-1} \left(\frac{19\lambda \left[e^{-\frac{20Gt}{19k\lambda}} \cos(Gt) - 1 \right] + 20k^{-1} e^{-\frac{20Gt}{19k\lambda}} \sin(Gt)}{-20k^{-1} \left[e^{-\frac{20Gt}{19k\lambda}} \cos(Gt) - 1 \right] + 19\lambda e^{-\frac{20Gt}{19k\lambda}} \sin(Gt)} \right) \quad [4b]$$

where
$$D' = \frac{5(19\lambda + 16)}{4(1+k\lambda) \sqrt{(19\lambda)^2 + (20k^{-1})^2}} \quad [5]$$

is the equilibrium value of the deformation parameter obtained as $t \rightarrow \infty$. Similarly, the equilibrium α obtained from equation [4b] by letting $t \rightarrow \infty$ is

$$\alpha = \pi/4 + 1/2 \tan^{-1} \left(\frac{19k\lambda}{20} \right) \quad [6]$$

If D' and D are always taken to be positive, it can be shown from equations [4b] and [6] that

$$\pi/4 \leq \alpha' \leq 3\pi/4; \quad [7a]$$

$$\pi/4 \leq \alpha \leq \pi/2. \quad [7b]$$

Equations [4] show that if the fluid is suddenly sheared from rest the drop will undergo a transient motion which will appear as a damped "wobble" having a relaxation time τ , approximately given by

$$\tau = \frac{\lambda k}{G} = b \eta_{1/2} \quad [8]$$

For the case of zero interfacial tension, considered in the experimental work described below, $k = \infty$ and $\tau = \infty$. Here, when the drop is much more viscous than the medium, $\lambda \rightarrow \infty$, there is no damping and equations [4] reduce to

$$D' = \frac{5}{2\lambda} \sin \left(\frac{Gt}{2} \right), \quad [9a]$$

$$\alpha' = 1/4 [\pi (1-2n) + Gt]; \quad [9b]$$

$$\text{where } 2\pi n \leq Gt \leq 2\pi (n+1), \quad [9c]$$

and n is any integer greater or equal to zero. This condition is illustrated in Figure 2 where it may be seen that the initial orientation angle $\alpha' = 45^\circ$, and that with time, both α' and D' increase until a maximum value for the deformation, $D' = 5/2\lambda$ is reached at $\alpha = 90^\circ$. At this point there is a steady decrease in D' until it assumes its initially spherical shape while α' continues to increase to a maximum value of 135° . A further increase in time results in a cyclical repetition of the above phenomena, with the period of oscillation $T_0 = 2\pi/G$.

For the special case of $\sigma_{12} = 0$, $\lambda = 1$, corresponding to an initially spherical domain of pure medium the drop is stretched into an ellipsoid whose equation is:

$$x_1^2 + x_2^2 + (x_3 - Gtx_2)^2 = b^2, \quad [10]$$

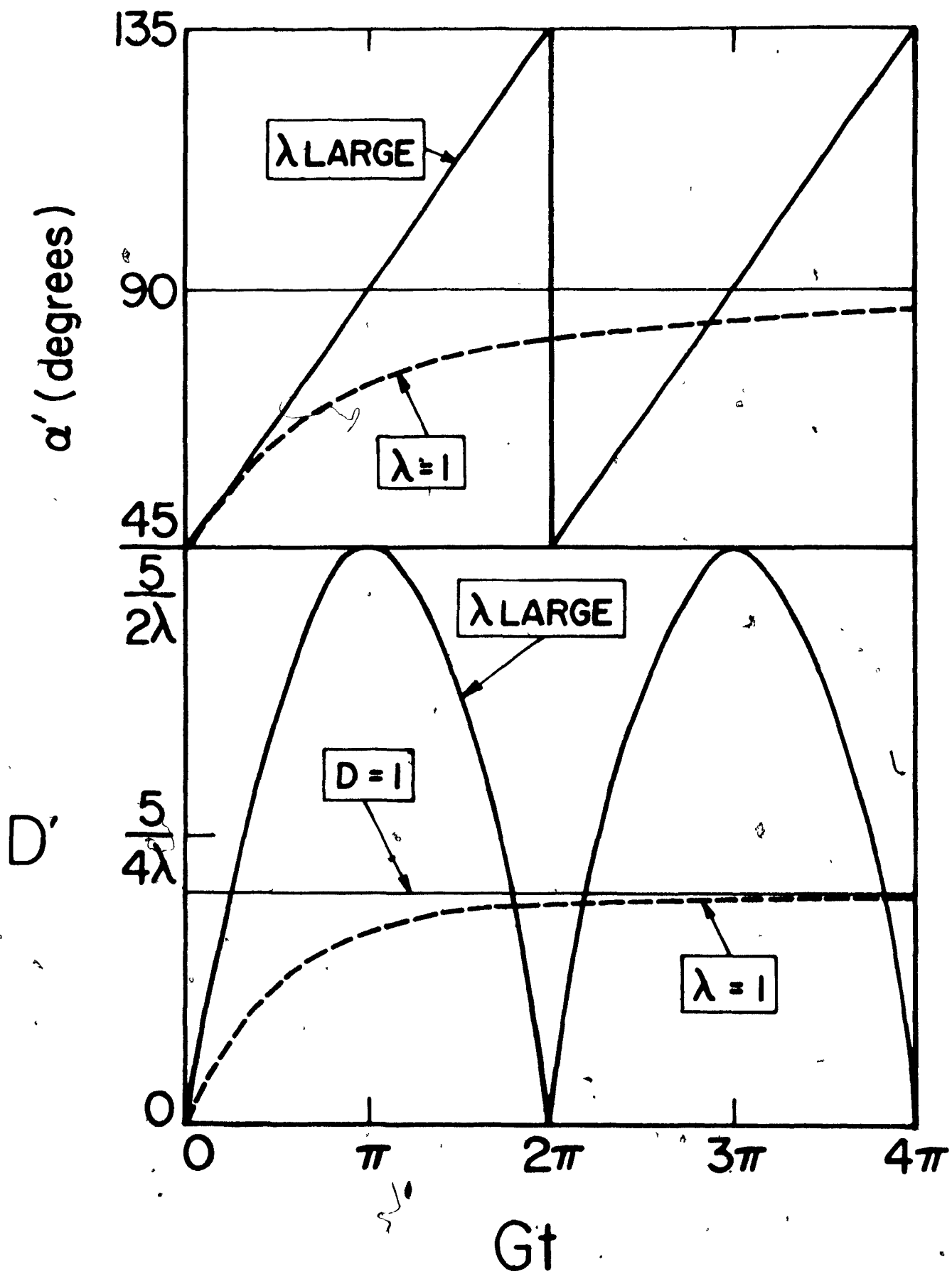
from which it can be shown that the following values of D' and α' are obtained ⁵⁾:

$$D' = \frac{\sqrt{G^2 t^2 \cos^2 \alpha' + 1 + 2Gt \sin \alpha' \cos \alpha'} - \sqrt{G^2 t^2 \cos^2 \alpha' + 1 - 2Gt \cos \alpha' \sin \alpha'}}{\sqrt{G^2 t^2 \cos^2 \alpha' + 1 + 2Gt \sin \alpha' \cos \alpha'} + \sqrt{G^2 t^2 \cos^2 \alpha' + 1 - 2Gt \sin \alpha' \cos \alpha'}} \quad [11]$$

$$\text{where } \alpha' = \frac{\pi}{4} + \frac{1}{2} \tan^{-1} \left(\frac{Gt}{2} \right) \text{ with } 0 \leq \tan^{-1} \left(\frac{Gt}{2} \right) \leq 90^\circ. \quad [12]$$

Figure 2 The undamped oscillations of a soluble drop (λ large) suddenly subjected to a shear field. Both the drop deformation D' and orientation angle α' , calculated from Equations [9], have a period of oscillation $T_0 = 2\pi/G$. The steadily increasing D' and α' to asymptotic values of 1.00 and 90° for $\lambda = 1$ calculated from Equations [11] and [12] are shown as broken lines.

(After Torza, Cox and Mason)



The dashed line in Figure 2 shows this monotonic increase of D' and α' predicted from equations [11] and [12]. A similar continuous increase in deformation and orientation is predicted for all values of $\lambda < 1$.

Fair agreement of the measured transient deformation and orientation of drops in Newtonian systems of silicone oils, polyglycol and castor oils having interfacial tensions > 0 , with that predicted by the above theory has been obtained⁵⁾. In general, however, the measured D' and α' and the period of oscillation were found to be somewhat greater than predicted. These differences were ascribed to the relatively higher transient deformations which produced longer periods of oscillations since the deformed drop required more time to rearrange its shape, and also to the fact that the theory is strictly only applicable at values of D' close to zero.

b) Break-up of drops

In the original treatment, Taylor suggested⁸⁾ that when the difference in normal stresses at the interface exceeded the surface tension forces tending to restore the drop shape, the drop will burst, and that should occur at a deformation $D_B \sim 1/2$. He demonstrated the existence of three classes of burst depending on the value of λ , of which one, that at high λ did not involve actual break-up of the particles, which instead aligned themselves with the flow, $\alpha \approx \pi/2$, at a limiting deformation. Subsequent experimental work^{1,12)} confirmed these results, adding a sub-group to the original class B break-up ($\lambda \sim 1$). The 3 modes of burst are illustrated

in Figure 3, taken from the work of Rumscheidt and Mason¹²⁾.

More recent work⁵⁾, however, demonstrated that drops exhibiting class A break-up ($\lambda < 0.2$) in which the particles develop pointed ends from which fragments of the drop phase are ejected, are in unstable equilibrium as a result of high dG/dt . When the velocity gradient was increased very slowly, class B-1 break-up, in which the drops neck-off in the middle, was observed in systems of low λ . Type B-1 break-up at low dG/dt was in fact noted for systems having λ from 10^{-3} to 3.0, above which value of λ , no break-up occurred.

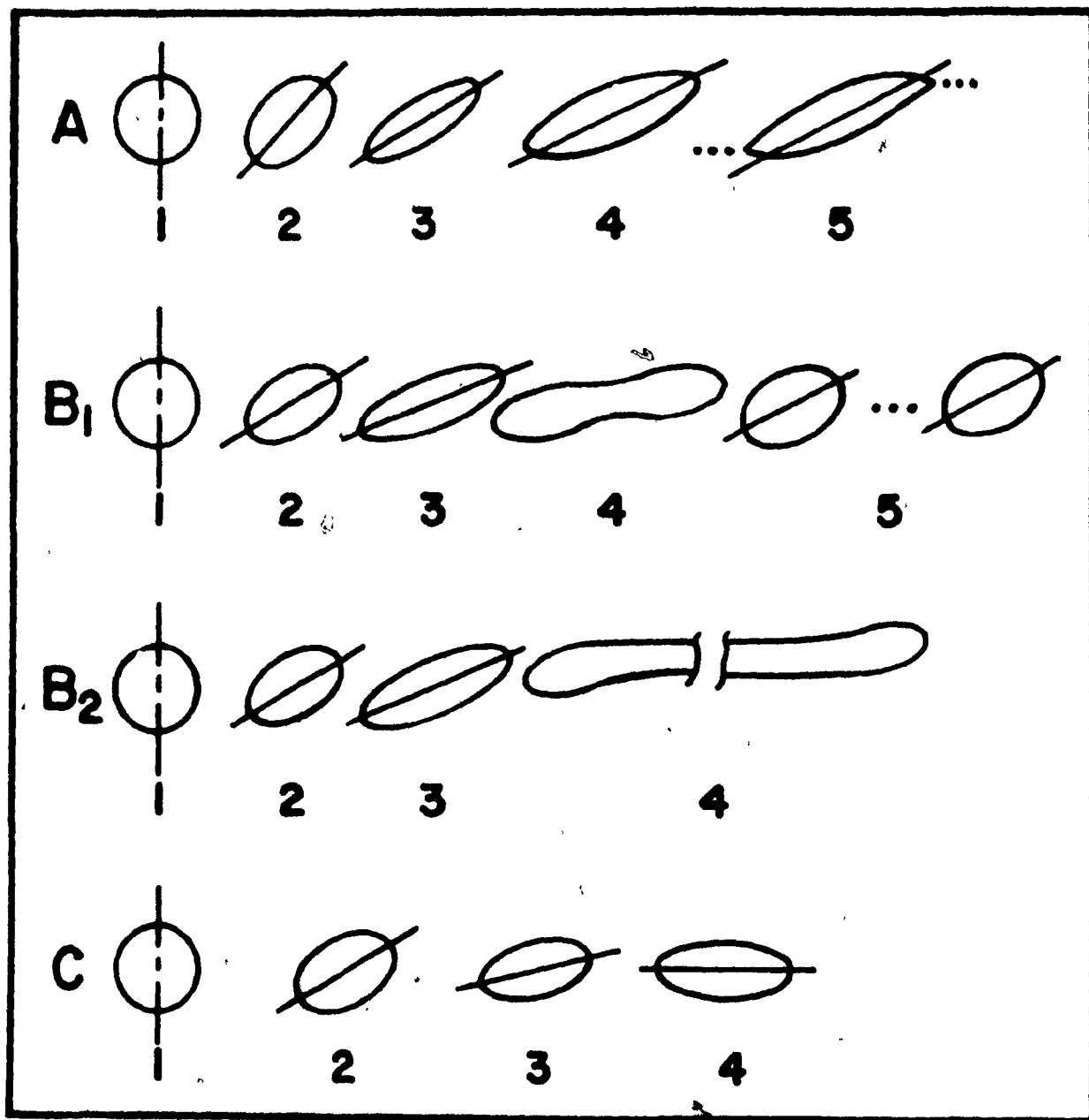
Other workers^{4,13,14)} have investigated the behaviour of Newtonian drops in non-Newtonian media and non-Newtonian drops in Newtonian media. Similar results to those obtained in completely Newtonian systems were observed for the deformation, orientation and break-up with the exception of suspended viscoelastic drops in a Newtonian fluid, where the deformation was smaller than the theoretical.

4. EXPERIMENTAL PART

a) Apparatus

The Couette apparatus used (Mark. IV) consisted of two counter-rotating plexiglass cylinders connected to continuously variable speed drives¹⁶⁾ and the particle motions in the annulus could be viewed either along the X_1 - or X_2 - axis of the shear field (see Appendix). In order to ensure that the translational velocity of the drops were initially zero when rotation of the cylinders suddenly

Figure 3 Tracing from photographs of drops, in shear fields described by Rumscheidt and Mason, illustrating the behaviour of drops in shear flow up to burst. Shown are: Class A ($\lambda < 0.2$); Class B₁ and B₂ ($0.03 \leq \lambda \leq 2.2$); Class C ($\lambda > 3.8$). It was reported that the three classes were related to λ but that there were no sharp boundaries between them.



commenced, they were inserted into the suspending fluid using a long capillary needle attached to a syringe placed at the radial position of the previously determined stationary layer. However, with the appreciable lateral migration of deformable particles suspended in non-Newtonian liquids under the conditions of the experiments, movement of the drop out of the stationary layer soon occurred.

Particle deformation and break-up over a range of shear rates from 0 to 20 sec^{-1} were viewed through a microscope aligned either along the X_1 - or X_2 - axis and the events recorded by means of a Paillard Bolex camera. The cine films were subsequently analyzed by projecting them onto a drafting table.

b) Fluids

The Newtonian liquids employed in this study were silicone oils (Dow Corning 200 series) having viscosities from 10 to 500 poise at $21^\circ \pm 0.5^\circ\text{C}$. The pseudoplastic solutions were obtained by dissolving a carboxyvinyl polymer (carbopol 940, B.F. Goodrich Chemical Co.) in water at concentrations ranging from 0.05% to 0.15% w/v. Beside the viscoelastic solutions of polyacrylamide in water (Cyanamer P250, American Cyanamide Company) at concentrations from 1% to 5% w/v and polyisobutylene in Decalin (Vistanex, Enjay Company, New York, New York) in the range 2.5% to 5% w/v, aqueous guar gum solutions (Jaquar A20D, Stein-Hall Ltd., Toronto, Ontario) at concentrations up to 1.5% w/v were also utilized.

Since the experiments involved the deformation of drops in systems having zero or near zero interfacial tensions, the phase boundary was often not clearly visible. Guanine particles were therefore added to the drop phase so that it could more easily be seen. The viscosities of the Newtonian silicone oils were measured in a rotational viscometer (Epprecht Rheomat 15); no difference in the values of η_0 were detected after the addition of guanine marker particles.

The apparent viscosity, normal stress differences and the elastic properties of the carbopol, P.A.A. and P.I.B. solutions used have been given in the previous chapter of this thesis.

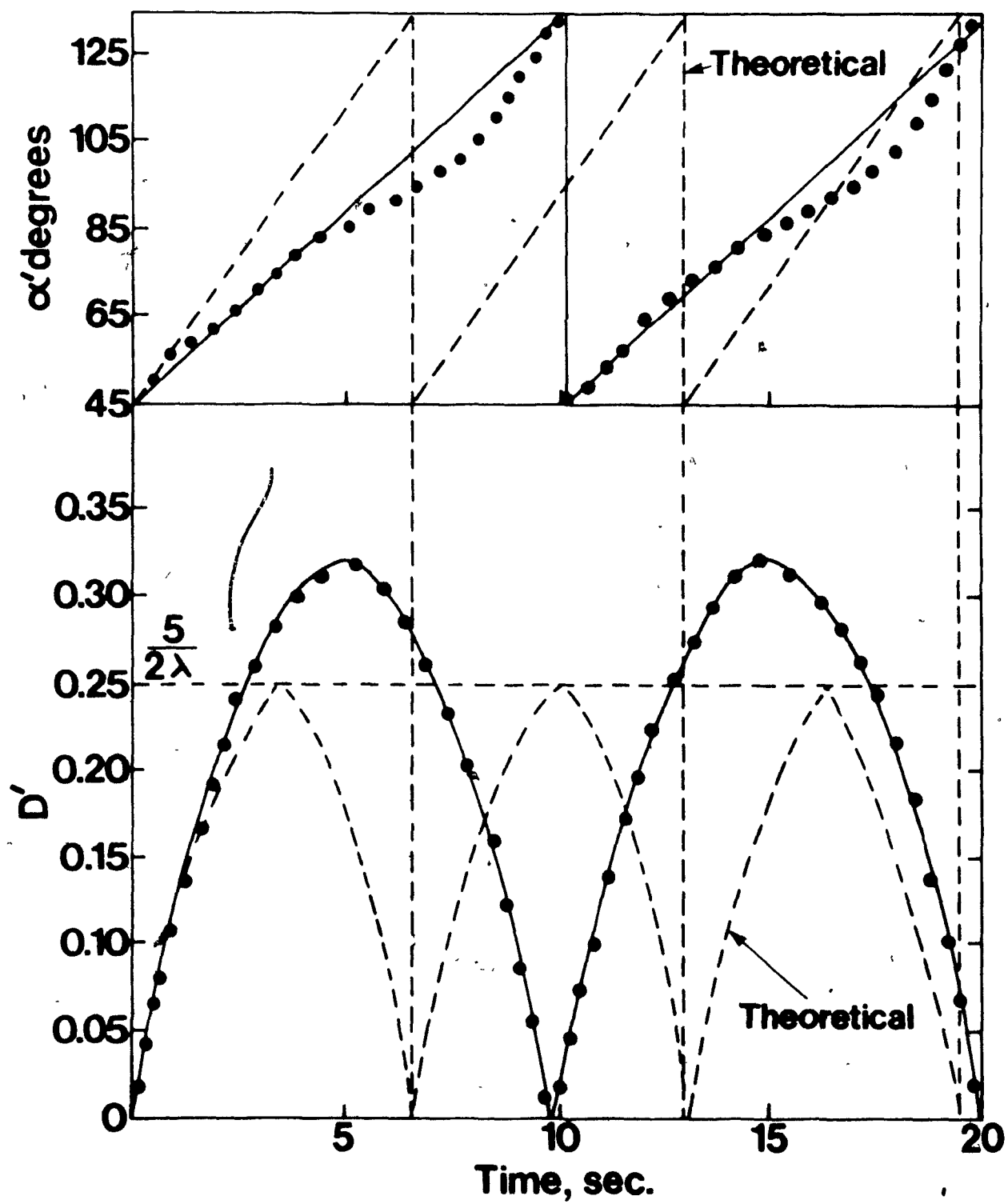
5. RESULTS AND DISCUSSION

a) Drop deformation in Newtonian systems, $\sigma_{12} = 0$

Systems using pairs of silicone oils in which the viscosity ratio was varied from 0.02 to 50 were used to test the theory outlined in Section 2.

(i) High viscosity ratios. A typical result, obtained with a 200 poise silicone oil drop in a 20 poise silicone oil at $G = 0.974 \text{ sec}^{-1}$, is shown in Figure 4. Little or no damping of the wobble was observed, but as can be seen the measured period of oscillation T_0 was appreciably longer than that calculated from equation [9c] and D' greater than predicted from equation [9a]. The orientation α' increased from an initial value of 45° to 135° as predicted, but at a rate

Figure 4 Showing the undamped oscillation for a soluble drop ($\lambda = 10$). Drop viscosity = 200 poise, medium viscosity = 20 poise (Dow Corning silicone oils, 200 series). $G = 0.947 \text{ sec}^{-1}$. Both the theoretical drop deformation D' ($5/2\lambda = 0.25$) and the orientation angle α' are calculated from Equation [9], have a period of oscillation $T_0 = 2 \pi/G = 6.45 \text{ sec}$.



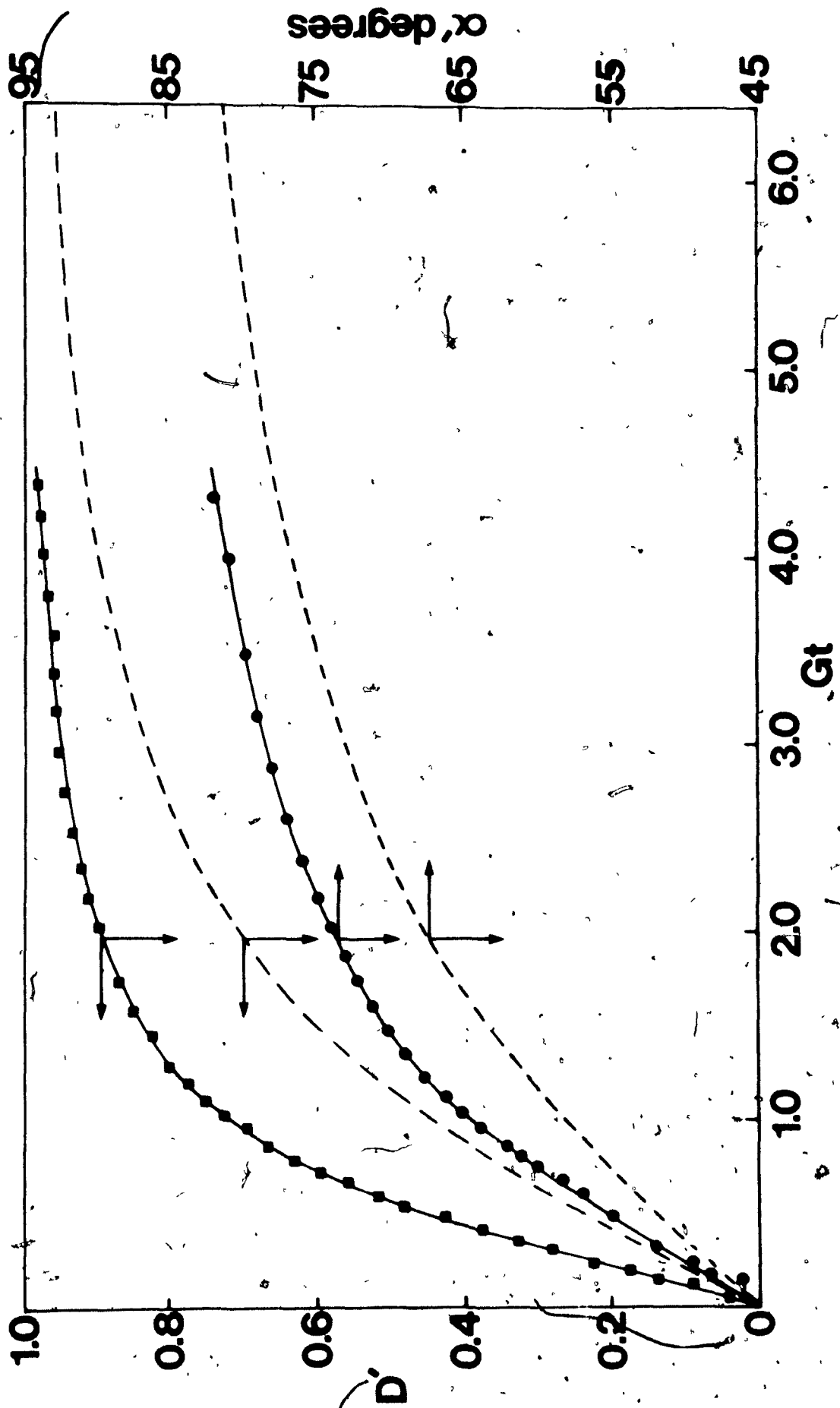
which fluctuated somewhat. Although the measured T_0 were always greater than the theoretical values, the transient deformations exhibited a scatter within the same system, being mostly greater but sometimes also smaller than the predicted values. This result probably reflected an error inherent in the experimental method viz. the difficulty of producing a spherical drop in a system of zero interfacial tension. It was thus likely that one sometimes observed a time dependent deformation D' superimposed on the 'deformation' of an initially non-spherical drop.

(ii) Low viscosity ratios. The prediction of the theory under these conditions is that the deformation and orientation increase monotonically from 0 and 45° to 1 and 90° respectively i.e. the drop becomes indefinitely extended and aligned with the flow. This is borne out experimentally in systems having $\lambda = 0.25$ and 0.5 , although both the time dependent deformation and orientation were found to be greater than the theoretical values predicted by equations [1b] and [12]. Figure 5, illustrates the variation of deformation and orientation for a silicone oil $\eta_1 = 50$ poise in a medium $\eta_2 = 100$ poise at a shear rate $G = 0.022 \text{ sec}^{-1}$.

b) Drop deformation in viscoelastic systems

Here the fluids used consisted of pairs of aqueous P.A.A. solutions giving $\sigma_{12} = 0$, and drops of aqueous guar gum solutions suspended in an aqueous polyacrylamide media. Systems of high and low viscosity ratio were made up having σ_{12} close to zero.

Figure 5 Plot of the drop deformation D' and orientation angle α' against Gt for a soluble drop ($\eta = 50$ poise) suspended in a medium ($\eta = 100$ poise) [Dow Corning 200 series]. $G = 0.0215 \text{ sec}^{-1}$. The dotted line shows the theoretical curves calculated from Equations [11] and [12].

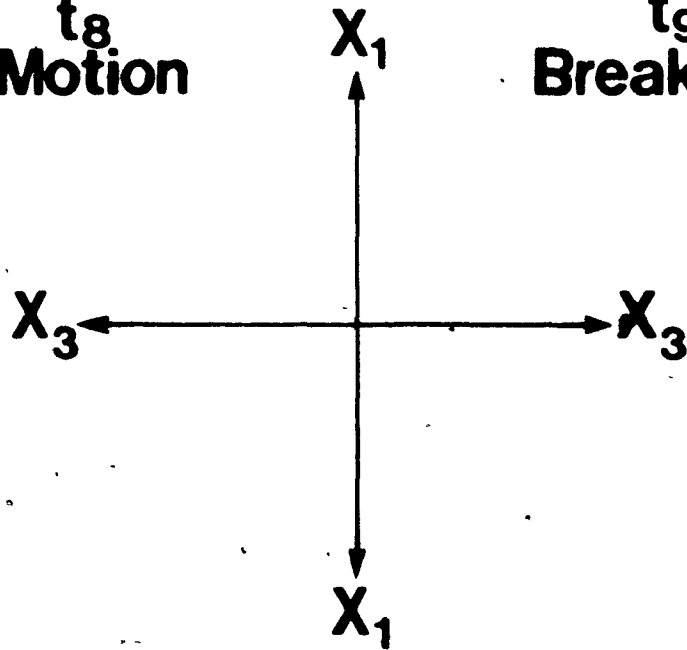
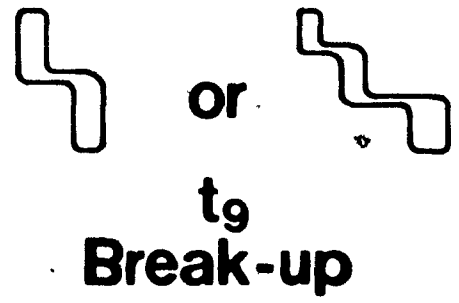
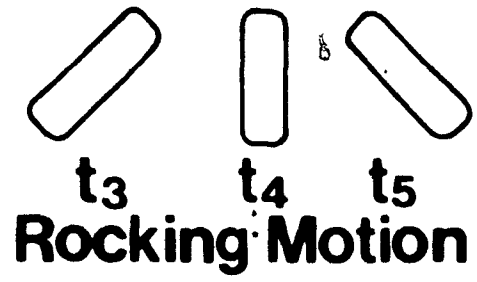
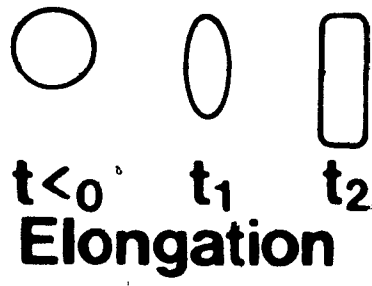


(i) High viscosity ratios. When the combinations of polyacrylamide solutions were viewed along the vorticity (X_1 -) axis, a rather complex mode of deformation and break-up was observed upon shearing. A somewhat clearer picture, however, emerged when the same events were viewed in a direction normal to the planes of shear i.e. along the X_2 -axis. The initially spherical drop became extended vertically (along the X_1 -axis) into a cylindrical shape. This then exhibited a rocking motion from side to side about the X_1 -axis, somewhat reminiscent of rotation in a spherical elliptical orbit of a rod in Couette flow when viewed along the X_2 -axis¹⁶). As the longitudinal deformation continues a buckling motion sets in, which progresses to the mode of break-up schematically shown in Figure 6.

Although the time to break-up in a given system decreased with increasing shear rate, the mode of extension of the drop and final burst were identical even at G as low as 0.05 sec^{-1} . Moreover, when shear continued after break-up, the daughter droplets in turn exhibited the same longitudinal deformation into cylinders and the break-up illustrated in Figure 6, thus giving one a large number of very small cylindrical droplets which eventually were completely mixed with the medium. It thus appears that this method of deformation and break-up is independent of drop size.

Similar behaviour was observed with the guar gum drops in P.A.A. solutions, except that here the cylinders became varicose and necked off at intervals along their length as the deformation continued. This effect is probably due to the existence of a finite interfacial tension in the system.

Figure 6 Schematic representation of the deformation and break-up procedure for a viscoelastic drop suspended in a viscoelastic medium with zero or near-zero interfacial tension and high viscosity ratio subject to Couette flow.



In order to ascertain whether the above observed vertical deformation into cylinders was an effect due solely to the viscoelastic properties of the two liquids or whether it was a combination of viscoelasticity and zero or very low interfacial tension, a drop of 5% polyisobutylene in Decalin solution was suspended in 3% P.A.A. solution, $\lambda \sim 2$. It was observed that the deformation and burst over a range of G from 0.05 to 5 sec^{-1} followed class B-1, i.e. when shear was suddenly imposed, the drop extended into an ellipsoid at low G ; at higher G it was further pulled out into a thread which above a certain critical value of the gradient necked off and formed two large droplets separated by tiny satellite droplets. If the shear was slowly increased with time the same progressive deformation and break-up occurred.

(ii) Low viscosity ratios. Here, the drops in the polyacrylamide and guar gum/P.A.A. systems were drawn out into infinitely long threads, a behaviour similar to that in silicone oils previously described, where D' and α' tend monotonically to 1.00 and 90° respectively.

c) Pseudoplastic drop in viscoelastic medium

The system consisted of aqueous Carbopol drops suspended in aqueous polyacrylamide solutions, both high and low viscosity ratios. The observed mode of deformation here was independent of the viscosity ratio: both at high or low λ , the initially spherical drop, upon suddenly being sheared, deformed into an ellipsoid from which continuous threads of liquid were withdrawn from the pointed ends. Thus, the drop,

while retaining its ellipsoidal shape, gradually diminished in size with time. The continuous ejection of a thread, rather than that of discrete droplets as in type A break-up previously found in Newtonian systems^{1-3,5)} as well as for pseudoplastic drops in Newtonian media⁴⁾ is most probably due to the low value of the interfacial tension in the systems used here.

6. CONCLUDING REMARKS

This Part presents the results of a preliminary investigation into the deformation and break-up of liquids drops having zero or near zero interfacial tension with the suspending medium. The observations employing Newtonian liquids were found to be in fair agreement with the proposed theory⁶⁾ taking into consideration the difficulty in obtaining a perfectly spherical drop. The astonishing deformation and break-up of two mutually soluble viscoelastic liquids, when the drop is much more viscous than the medium, however, cannot be explained at present, although by comparison of the results using pseudoplastic drops and also viscoelastic drops where σ_{12} was finite, it appears to be due to a combination of the elasticity of the system and the zero interfacial tension. It is interesting to note here the behaviour of an elastomeric filament suspended in a Newtonian fluid, which when subject to Couette flow under certain conditions orients itself similar to a corkscrew rotating around the vorticity (X_1 -) axis¹⁷⁾.

LIST OF SYMBOLS

b	= radius of the spherical drop
B, L	= minor and major axis of deformed drop
$D'; D; D_B;$	= $(L-B)/(L+B)$, transient drop deformation; steady value; value at burst.
G	= velocity gradient
k	= $(Gb\eta_2/\sigma_{12})$
r, ϕ, σ	= spherical polar coordinates
t	= time
T_0	= period of oscillation
u_3	= velocity along X_3 -axis
X_1, X_2, X_3	= Cartesian coordinate axes of external flow field

GREEK

$\alpha; \alpha'$	= steady orientation angle; transient value
η_1, η_2	= viscosity of drop and medium respectively
λ	= η_1/η_2 , viscosity ratio
σ_{12}	= interfacial tension
τ	= relaxation time defined by Equation [8]

REFERENCES

1. Bartok, W. and Mason, S.G., J. Colloid Sci., 13, 293, (1958).
2. Rumscheidt, F.D. and Mason, S.G., J. Colloid Sci. 16, 210 (1961).
3. Chaffey, C.E., Brenner, H. and Mason, S.G., Rheol Acta, 4, 56 (1965).
4. Gauthier, F., Goldsmith, H.L. and Mason, S.G., Trans. Soc. Rheol. 15, 297, (1971).
5. Torza, S., Cox, R.G. and Mason, S.G.,
6. Cos, R.G., J. Fluid Mech. 37, 601 (1969).
7. Taylor, G.I., Proc. Roy. Soc. (London), A138, 41 (1932).
8. Taylor, G.I., Proc. Roy. Soc. (London), A146, 401 (1934).
9. Chaffey, C.E. and Brenner, H., J. Colloid and Interface Sci.
10. Cerf, R., J. Chimie Phys., 48, 59 (1951).
11. Turner, B.M. and Chaffey, C.E., Trans. Soc. Rheol., 13, 411 (1969).
12. Rumscheidt, F.D. and Mason, S.G., J. Colloid Sci., 16, 238 (1961).
13. Flumerfelt, R.W., Ind. Eng. Chem. Fundam. 11, 312 (1972).
14. Karnis, A. and Mason, S.G. Trans. Soc. Rheol., 10, 571 (1967).
15. Darabaner, C.L., Roasch, J.K. and Mason, S.G., Canad. J. Chem. Eng., 45, 3 (1967).
16. Trevelyan, B.J. and Mason, S.G., J. Colloid Sci. 6, 354 (1951).
17. Forgacs, O.L. and Mason, S.G., J. Colloid Sci., 14, 473 (1959).

PART IV

1. GENERAL CONCLUSIONS
2. SUGGESTIONS FOR FURTHER WORK
3. CLAIMS TO ORIGINAL RESEARCH

GENERAL CONCLUSIONS

The main findings and conclusions arising from the work described in this thesis may be summarized as follows.

a) Rigid Particles

The angular velocities of rigid particles in the pseudoplastic liquids were in agreement with Jeffery's¹⁾ equations whereas with the viscoelastic fluids there was a pronounced increase in the period of rotation. Rods and discs drifted into limiting rotational orbits of $C = 0$ and $C = \infty$ respectively, when suspended in pseudoplastic fluids. However, discs in viscoelastic media drifted to an equilibrium orbit where $0 < C < \infty$, and although the rotation was periodic the value of C varied from a maximum at $\phi_1 = 0, \pi$ and a minimum at $\phi_1 = \pi/2, 3\pi/2$. At sufficiently high shear rates discs of $r_p \leq 0.007$ ceased to rotate and aligned themselves with the direction of the flow. A similar phenomenon was observed with rods under certain conditions, although in this case the equilibrium position of alignment with the flow was a metastable one. For rods suspended in viscoelastic liquids in which the drift in orbit was towards $C = 0$, four distinct stages of behaviour could be discerned in this movement towards the equilibrium position.

The results suggest that it was the first normal stress which was responsible for the orbit drift in these solutions, whereas the difference in particulate behaviour in

the two types of non-Newtonian media was attributed to the presence of elastic forces in the viscoelastic fluids.

b) Deformable Particles

Fair agreement with the theory proposed by Cox²⁾ was found with Newtonian systems where the drop and medium were miscible, for viscosity ratios above and below unity. For viscoelastic pairs when $\lambda \ll 1$, deformation was found to proceed such that the drop became cylindrical in shape aligned with its long axis in the X_1 -direction, the subsequent burst forming two or more daughter cylinders. Results suggested that this method of mixing was due to the elastic properties of the liquid and the zero interfacial tension. Mutually soluble pseudoplastic drops in viscoelastic media were found to follow the class A mode of deformation and burst, with the difference, that instead of discrete droplets being ejected from the pointed ends, continuous threads of liquid were withdrawn, this presumably being a consequence of the very low interfacial tension.

2. SUGGESTIONS FOR FURTHER WORK

In light of this and previous studies in this laboratory, the following suggestions are made for further investigations.

- i) Formulation of a theory to predict particle behaviour in non-Newtonian media.

ii) Experimental investigation of single particle behaviour in other types of non-Newtonian fluids such as plastic and dilatant fluids and Molten polymers, along with a full description of the rheological properties of these liquids.

iii) Determination of the stream lines around rigid and deformable particles in non-Newtonian fluids.

iv) Study of deformable particles, having zero interfacial tension with respect to the medium, in tube flow.

v) Determination of the critical value of the viscosity ratio λ below which no wobble occurs for a miscible liquid drop ($\sigma_{12} = 0$).

vi) Further experimental work to correlate particle behaviour with known rheological parameters of the suspending fluid.

vii) Investigation on the effect of a slowly increasing interfacial tension for non-Newtonian drops suspended in non-Newtonian media. With a view to defining the mixing or blending procedures in these systems.

viii) Experimental studies of optical anisotropy resulting from preferred orientations in flowing suspensions of cylinders.

3. CLAIMS TO ORIGINAL RESEARCH

i) Rigid particles suspended in viscoelastic fluids show a pronounced increase in the period of rotation from that given by Jeffery's theory¹⁾.

ii) Discs in viscoelastic media drift in orbit where $0 < C < \infty$.

iii) Rods in viscoelastic solutions, under certain conditions, can align themselves in the plane of shear and cease to rotate. It was found, however, that this was a metastable equilibrium position.

iv) Establishment of four distinct stages in the drift in orbit towards $C = 0$ for rods suspended in viscoelastic liquids.

v) Fair agreement was found with the proposed theory²⁾ for the behaviour of miscible liquid drops ($\sigma_{12} = 0$) in Newtonian systems.

vi) A novel cylindrical deformation was observed for miscible drops in completely viscoelastic systems.

97-

REFERENCES

1. Jeffery, G.B., Proc. Roy. Soc. (London) A102, 161 (1922).
2. Cox, R.G., J. Fluid Mech., 37, 601 (1969).

APPENDIX**THE COUETTE DEVICES**

APPENDIX

Principles and description of the Couette devices(a) Principles

Both Couette devices consisted of two concentric counter-rotating, vertical cylinders which establish laminar shear of the liquid contained in the annular gap. Due to the curvature of the cylinders, the velocity gradient $G(R)$ across the annulus is not constant and has a minimum value at the outer cylinder and a maximum at the inner cylinder¹⁾ (see Figure 1). The velocity gradient at the stationary layer for a Newtonian liquid is given by¹⁾,

$$G(R) = \frac{2(R_1^2 \Omega_1 + R_2^2 \Omega_2)}{R_2^2 - R_1^2} . \quad [1]$$

Here, R is the radial distance from the centre of rotation, R_1 and R_2 the radii of the inner and outer cylinders respectively and Ω_1 and Ω_2 their corresponding angular velocities. The latter being calculated from the speeds of rotation of the motors as measured by two direct reading tachometers. The velocity gradient at the stationary layer $G(R)$, after calibration, can be determined from the following relationship:

$$G(R) = k_1 N_1 + k_2 N_2 , \quad [2]$$

where N_1 and N_2 are the tachometer readings and k_1 and k_2 constants which vary with varying cylinder diameters.

(b) Description

The experiments employing the use of an electric field were performed in the Couette Mark II (see Figure 2), the rest of the work being carried out in the Couette Mark IV (see Figure 3).

(i) Couette Mark II²⁾. The two concentric cylinders were of stainless steel, the bottom of the outer cylinder being plate glass enabling illumination and viewing of the events along the X_1 -axis. The internal diameter of the outer cylinder was 15.24 cm and the inner cylinder had an outside diameter of 13.25 cm.

The independent motor drives were $\frac{1}{2}$ H.P., d.c. with magnetic amplifier control (Bepco Canada Ltd.) and were connected to the cylinders through 4-speed gear boxes (1:400, 1:100, 1:20, 1:5) giving a continuously variable shear rate up to 40 sec^{-1} .

A Paillard Bolax Reflex 16mm cine camera was mounted on a column which permitted movement in the vertical direction. This was attached to a platform which could be rotated either manually or electrically, through 120° about the X_3 -axis of rotating cylinders. A compound slide device also permitted adjustment in the X_2 and X_3 -directions.

(ii) Couette Mark IV. This device is essentially the same as that above, having motors, gear boxes and camera mountings identical to those of the Mark II. However, this machine can facilitate not only cylinders, but also parallel



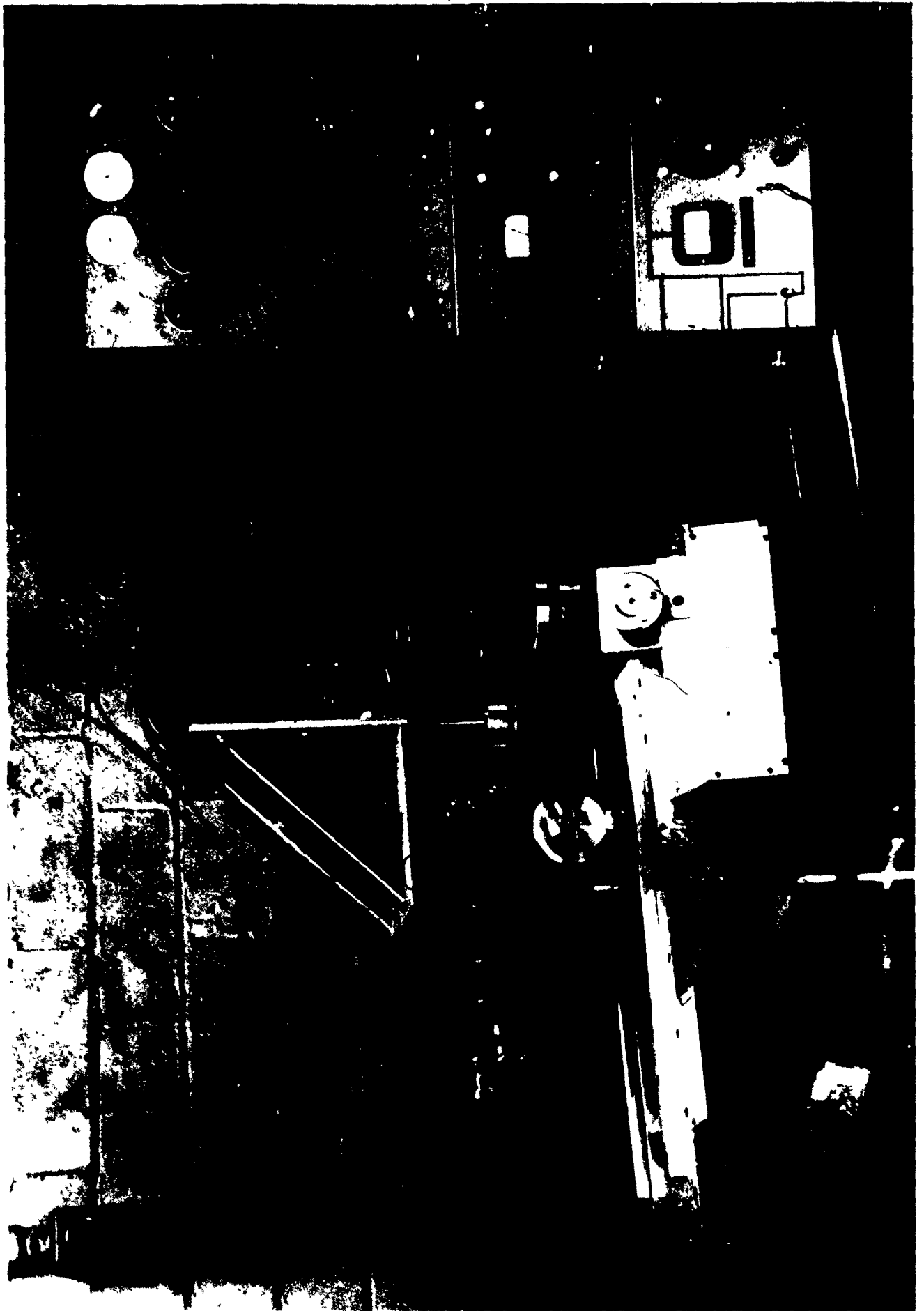


plate and cone and plate fixtures³⁾, which are mounted on concentric, counter-rotating spindles.

In this study, various sets of transparent cylinders (Plexiglas) were employed, thus allowing observation of the events along the X_1 - and X_2 -direction.

REFERENCES

1. Trevelyan, B.J. and Mason, S.G., J. Colloid Sci. 6, 354 (1951).
2. Bartok, W. and Mason, S.G., J. Colloid Sci. 12, 243 (1957).
3. Darabaner, C.L., Raasch, J.K. and Mason, S.G., Can. J. Chem. Eng. 45, 3 (1967).